Inorganic Chemistry

Article

pubs.acs.org/IC

A Family of Tri- and Dimetallic Pyridine Dicarboxamide Cryptates: Unusual *O,N,O*-Coordination and Facile Access to Secondary Coordination Sphere Hydrogen Bonding Interactions

Gary L. Guillet,[†,⊥] Jesse B. Gordon,[†] Gianna N. Di Francesco,[†] Matthew W. Calkins,[‡] Erik Čižmár,[§] Khalil A. Abboud,[†] Mark W. Meisel,[‡] Ricardo García-Serres,[∥] and Leslie J. Murray*[,†]

[†]Center for Catalysis, Department of Chemistry, University of Florida, Gainesville, Florida 32611-7200, United States

[‡]Department of Physics and the National High Magnetic Field Laboratory, University of Florida, Gainesville, Florida 32611-8440, United States

[§]Institute of Physics, Faculty of Science, P.J. Šafárik University, 04154 Košice, Slovakia

[∥]Laboratoire de Chimie de Biologie des Métaux, UMR 5249, Université Joseph Fourier, Grenoble-1, CNRS-CEA, 17 Rue des Martyrs, 38054 Grenoble Cedex 9, France

Supporting Information

ABSTRACT: A series of tri- and dimetallic metal complexes of pyridine dicarboxamide cryptates are reported in which changes to the base and metal source result in diverse structure types. Addition of strong bases, such as KH or $KN(SiMe_3)_2$, followed by divalent metal halides allows direct access to trinuclear complexes in which each metal center is coordinated by a dianionic *N,N,N*-chelate of each arm. These complexes bind a guest K^+ cation within the central cavity in a trigonal planar coordination environment. Minor changes to the solvent and equivalents of base used in the syntheses of the triiron(II) and tricobalt(II) complexes affords two trinuclear clusters with atypical *O,N,O*-coordination by each pyridine dicarboxamide arm; the amide carbonyl O atoms are oriented toward the interior of the cavity to coordinate to each metal center. Finally, varying the base enables the selective synthesis of dinuclear nickel(II) and copper(II) complexes in which one pyridine dicarboxamide arm remains protonated. These amide protons are at one end of a hydrogen bonding network that extends throughout the internal cavity and terminates at a metal bound hydroxide, carbonate, or bicarbonate donor. In the dinickel complex, the bicarbonate cannot be liberated as CO_2 either thermally or upon sparging with N_2, which differs from previously reported monometallic complexes. The carbonate or bicarbonate ligands likely arise from sequestration of atmospheric CO_2 based on the observed reaction of the di(hydroxonickel) analog.

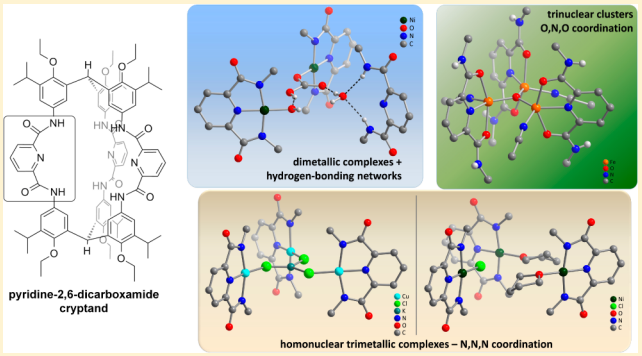

INTRODUCTION

Biological activation of small molecule substrates, such as O_2, CO_2, and N_2, typically occurs at metal clusters housed within the active site of metalloenzymes.[1] In these systems, redox cooperativity between metal ions and the high or intermediate spin states of the metal centers within the clusters are key requirements for the observed reactivity.[1b−d,p,2] Coupled to the properties inherent to the metal clusters, hydrogen bonding interactions within the secondary coordination sphere interact with and orient substrates to favor bond scission, redox events, or proton transfers.[1d,2c,3] Significant effort has focused on synthetic modeling of chalcogenide-bridged biological clusters (e.g., ferredoxins, oxygen-evolving complex) using either self-assembly,[4] in which the cluster is generated by the reaction of a low molecular weight ligand with a metal precursor, or by metalation of a ligand which preorganizes cluster assembly.[5] In the former approach, there is limited control of the cluster nuclearity or the coordination environment of each metal center, whereas the latter can suffer from poor tunability or low synthetic yields for the ligand.[5a,b]

In contrast to the sulfide- or oxide-bridged clusters, the diiron, tricopper, and heme-iron−copper active sites of the bacterial monooxygenases, multicopper oxidases, and cytochrome *c* oxidase, respectively, display weak interactions between the metal centers in the reduced state, but substrate binding activates cooperativity between the metal centers.[1a−e,p,2b,c,6] A number of groups have developed self-assembled and designed ligands to model these active sites;[6b,7] however, these systems display limited a priori control of the metal−metal distance or are unable to probe the role of proximal hydrogen bonding interactions. In addition, few

Received: December 1, 2014
Published: February 24, 2015

DOI: 10.1021/ic502873d
Inorg. Chem. 2015, 54, 2691−2704

examples have been reported in which hydrogen bonding interactions are incorporated into dinucleating ligands.[8]

Our focus has been on the use of macrobicyclic ligands to template the assembly of multimetallic complexes, wherein substrate binding within the internal void space facilitates electronic communication between the metal centers and leads to cooperative activation of substrates.[9] Here, we employ our previously reported cryptand, H_6**L**, composed of three pyridine dicarboxamide donor arms and two tri(5-ethoxyphenyl)-methane caps (Figure 1).[9a] In contrast to the monometallic

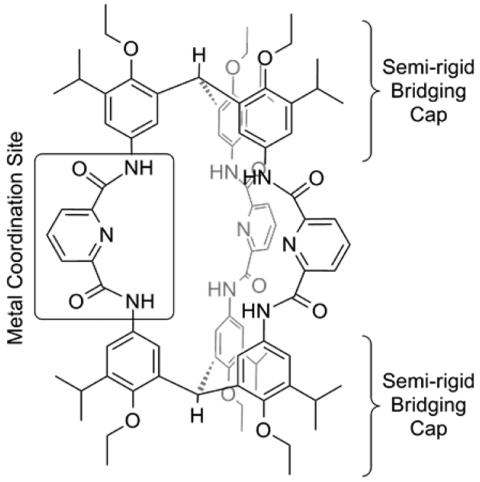

Figure 1. Structure of ligand H_6**L**.

pyridine-2,6-dicarboxamide (pyDCA) complexes in which bulky aryl substituents on the amide N atoms preclude formation of bis(pyDCA) compounds, the cryptand structure of H_6**L** provides the steric protection for each metal site, simultaneously positions the metal ions in close proximity, and, critically, ensures that the kinetically labile coordination sites are directed toward the internal cavity. Inspired by recent reactivity studies,[10] we aimed to expand our library of complexes to include divalent late 3d metal centers. Herein, we report the synthesis of trimetallic complexes of iron(II), cobalt(II), nickel(II), and copper(II), in which each metal is held within the *N,N,N*-chelate of each pyDCA arm. In addition, we report the characterization of two unexpected families of complexes derived from minor changes to our synthetic protocol for the trinuclear *N,N,N*-coordinated series. The first are the triiron and tricobalt complexes, in which each metal center is coordinated by the two amide O atoms and the pyridyl N atom of each arm, and these compounds represent uncommon examples of *O,N,O*-coordination by pyDCA donors. For the second, we observed that selective dimetalation of H_6**L** can be accomplished with copper(II) or nickel(II) to afford complexes containing a proximal hydrogen bonding network within the internal cavity.

RESULTS AND DISCUSSION

Synthesis, Characterization, and Reactivity of *N,N,N*-Coordinated Trinuclear Cryptates. As anticipated from our prior report,[9a] deprotonation of H_6**L** with a strong base followed by addition of a divalent metal halide indeed affords the corresponding trimetallic complexes in yields of 39%, 78%, 92%, and 62% for the tricopper(II) (**1**), triiron(II) (**2**), tricobalt(II) (**3**), and trinickel(II) (**4**) compounds. Upon metalation of the dianionic N_3-chelate of each pyDCA arm, we observe distinctive changes in the infrared spectra relative to the protonated ligand: there is a decrease in the intensity of the absorptions at 1670 and 1683 cm^{-1} and an increase in intensity at ~1600 cm^{-1} in the complexes relative to the free ligand, as well as strong absorption bands between 1590 and 1570 cm^{-1} for **1**−**3**. Minor differences from this general trend are observed in spectra of the trinickel(II) complex **4**; specifically, the presence of absorption bands at 1610, 1630, and 1590 cm^{-1} (Figures S1−S4, Supporting Information). These spectral changes are indicative of *N,N,N*-coordination of the bound metal centers and provide a facile method to aid in identifying the cryptand donor atoms in the reaction product (vide infra).

In the solid state structure of **1** (Figure 2), one of the two $[K(18\text{-crown-}6)]^+$ countercations stacks within a cleft between two pyDCA arms of the dianionic complex $[(CuCl)_3KL]^{2-}$ with the other two clefts occupied by solvent molecules (Supporting Information Figure S8). Each copper(II) center is held in a distorted square planar coordination environment (τ_4 = 0.14−0.20) composed of three pyDCA *N*-atoms and one

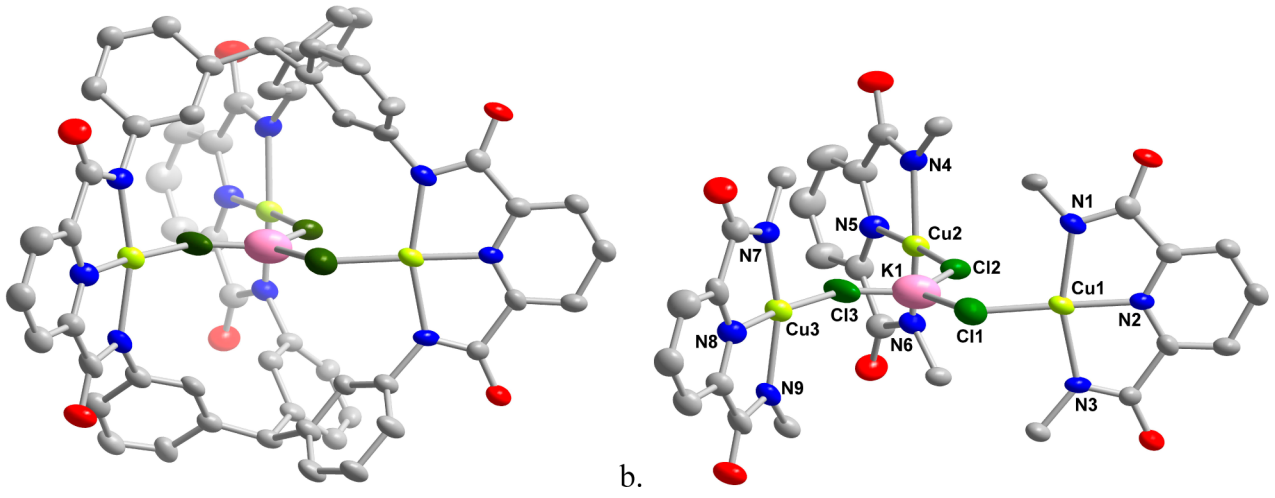

Figure 2. Solid state structure of **1** collected at 100 K (a) and cut away of the central cavity (b). C, N, O, Cu, K, and Cl atoms are represented as gray, blue, red, yellow-green, pink, and green ellipsoids (15%), respectively. Two $K[18\text{-crown-}6]^+$ ions, solvents of crystallization, H atoms, and OEt and iPr substituents have been removed for clarity.

DOI: 10.1021/ic502873d
Inorg. Chem. 2015, 54, 2691−2704

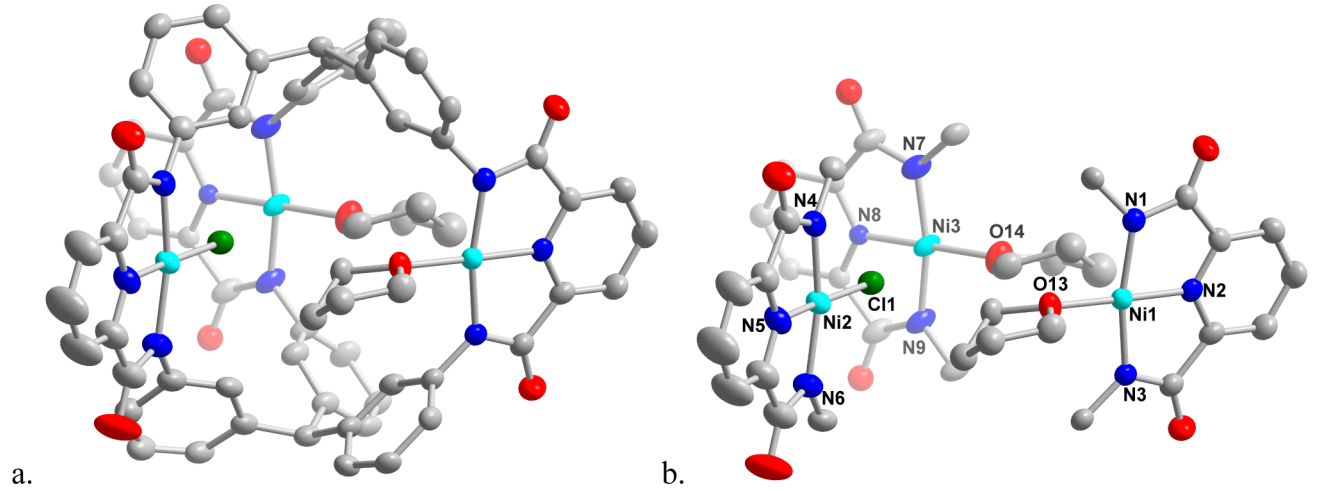

Figure 3. Solid state structure of **4** collected at 100 K (a) and cut away of the central cavity (b). C, N, O, Ni, and Cl atoms are represented as gray, blue, red, aqua, and green ellipsoids (70%), respectively. A K[18-crown-6]$^+$ cation, solvents of crystallization, H atoms, and OEt and iPr substituents have been removed for clarity.

chloride donor, and the copper(II) ions lie nominally out of the N_3Cl plane (<0.04 Å). As expected from the constraints placed on the complex by the cryptand ligand, there are a number of similarities between the structure of **1** and that reported for the triiron(III) complex, $[(FeCl_2)_3\mathbf{L}]^{3-}$.[9a] First, each metalated ligand arm is overall monoanionic as a chloride coordinates to each metal center. Whereas a number of monocopper(II) pyDCA complexes are solvent-adducts, **1** incorporates chloride donors instead of solvent in the fourth coordination site, presumably because the steric constraints enforced by the cryptand. Second, the plane of the pyridyl ring in each arm of **1** is twisted out of the plane of the aryl rings in each triphenylmethane cap (60.4−71.1°). This configuration results in the N_{pyr}−Cu vector of each arm oriented slightly away from the center of the internal cavity. Finally, the metal−metal distances in **1** (6.525−6.694 Å) are similar to those in the ferric complex (6.723 Å).[9a]

We were surprised that the tricopper(II) cryptate accommodates a guest K^+ ion, which is coordinated to only the Cl^- donors, instead of isolating the trianionic $[(CuCl)_3\mathbf{L}]^{3-}$ complex. The K^+−$arene_{cap}$ (4.865−5.128 Å) and K^+−H_{cap} (3.121−3.385 Å) distances are significantly longer than those usually observed for cation−π interactions,[11] which supports our assignment of a nominally three-coordinate K^+ ion. On the basis of prior reports of the nucleophilicity of the fourth (non *N*-atom) donor in mononuclear pyDCA compounds,[10a−g] the three chloride ligands likely create a favorable electrostatic pocket to interact with the alkali cation to stabilize the observed and unusual low coordination number. The synthetic approach for **1** also suggests that this alkali cation binding site is selective for K^+ over other cations and also has a higher affinity for K^+ than 18-crown-6. Specifically, sufficient equivalents of 18-crown-6 are present in the reaction mixture to account for each charge balancing K^+ for the expected complex $[(CuCl)_3\mathbf{L}]^{3-}$; yet, mass spectrometry, crystallography, and combustion analysis data provide evidence for formation of only $[(CuCl)_3K\mathbf{L}]^{2-}$. Moreover, our preliminary attempts to test this hypothesis by replacing $KN(SiMe_3)_2$ with $NaN(SiMe_3)_2$ in the synthesis of **1** do not appear to afford a complex with guest Na^+ cation, but rather $[(CuCl)_3\mathbf{L}]^{3-}$ is isolated. To our knowledge, **1** represents a unique example of a three-coordinate K^+ center and hints at a different design strategy for selective alkali cation receptors. Although our attempts to obtain single crystals of **2** and **3** of sufficient quality for X-ray diffraction analysis are ongoing, HRMS-ESI(−) data and combustion analyses of **1**−**3** support a parent ion formula consistent with the doubly charged anionic complex containing one K^+ cation, three transition metal ions, and three chloride ions (Figure S5−S7, Supporting Information). Given the similarities between the IR spectra of these three compounds and the apparent stability of the parent ion $[(MCl)_3K\mathbf{L}]^{2-}$, we tentatively assign **2** and **3** as isostructural complexes to **1**.

In contrast to data collected on complexes **1**−**3**, the trinickel complex was isolated as the monoanionic species $[(Ni(THF))_2(NiCl)\mathbf{L}]^-$ in the solid state (Figure 3). With respect to **1**, the $[K(18\text{-crown-}6)]^+$ counteraction is displaced from the cleft and stacks between the isopropyl groups in the cap, and two nickel centers coordinate solvent molecules rather than halide donors (Figures S8 and S9, Supporting Information). Two structural changes allow **4** to accommodate the THF donors and point to the unexpected flexibility of the ligand (Table S2, Supporting Information). First, the distance between the two central carbon atoms of the triphenylmethane caps contracts slightly in **4** (9.23 Å) as compared to **1** (9.59 Å), leading to a widening of the clefts between the cryptand arms and an average increase in the metal−metal distances (6.9 ± 0.3 Å in **4** vs 6.6 ± 0.1 Å in **1**). This increase in metal−metal separation is more evident in the ∼7 Å distance between the two THF-coordinated Ni^{II} centers in **4**. Second, the angle between the planes of the pyridyl rings coordinated to Ni1 and Ni3 and those of the adjacent aryl groups on the triphenylmethane caps are larger (73.4−86.5°) than the comparable angles in **1**, which results in the N_{pyr}−Ni vector being oriented further away from the central cavity of the ligand and toward the cleft. We cannot exclude the possibility that minor differences in the synthetic procedures of **1** and **4** might result in changes to product speciation or that one structure type selectively crystallizes depending on the metal identity. However, the subtle differences in the metal−ligand bond distances that are expected between the nickel and copper ions and each pyDCA arm could be amplified within the confines of the cryptand cavity. Specifically, the Ni−Cl bond distances are reported to be shorter than the comparable Cu−Cl distances in the monometallic complexes,[10a,h] which would afford a larger

DOI: 10.1021/ic502873d
Inorg. Chem. 2015, 54, 2691−2704

central cavity lined by the halide donors for a hypothetical $[(NiCl)_3\mathbf{L}]^{3-}$ complex. In addition, the tetragonal coordination environment around each copper center in **1** allows the chloride donor to be positioned slightly within the internal cavity (cf., N_{pyr}–Cu–Cl bond angles, Table S3, Supporting Information), which further contracts the chloride–chloride distances to likely favor K^+ binding. Regardless, the structures of **1** and **4** indicate that ligand flexibility can provide a pathway for halide exchange with substrates and product dissociation during reactions of the *N,N,N* family of complexes.

In cyclic voltammograms on solutions of **1** in DMF, we observe a quasireversible wave at $E_{1/2}$ = −0.043 V vs Fc^+/Fc (Figure 4), which is at a comparable potential to the redox

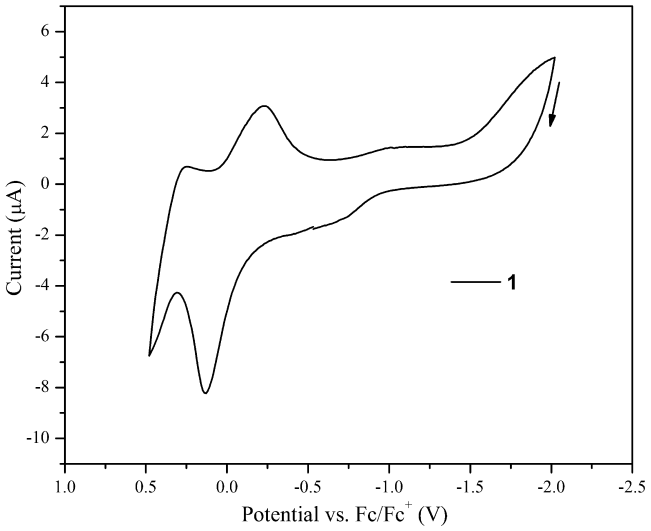

Figure 4. Cyclic voltammogram of **1** in DMF over a limited potential window at a scan rate of 100 mV/s. 0.1 M $TBAPF_6$ used as supporting electrolyte. Working electrode: 1 mm Pt button. Auxiliary electrode: Pt wire. Reference electrode: $Ag/AgNO_3$ in MeCN.

process assigned as the $Cu^{II/III}$ couple by Tolman and co-workers (−0.076 V vs Fc^+/Fc) for a monocopper(II)-hydroxide pyDCA complex.[10f] The wave observed here is broad, and no other redox events are present over the scanned potential window, indicative of minimal electronic communication between the metal centers. In contrast, two closely spaced but discernible redox events are present in voltammograms of **2** at $E_{1/2}$ = −0.152 and −0.422 V, and only ill-defined anodic and cathodic events are observed for **3** at 0.047 and −0.444 V (Figure 5). The redox processes for **2** are analogous to those for mononuclear ferrous (−0.490 V vs SCE) and ferric (−0.570 V vs SCE) pyDCA complexes[12] and are consistent with the pyridine-diimine[13] and pyridine-diamine[14] iron(II) compounds if the trend in donor strengths is considered. The richer redox chemistry of **2** is surprising as compared to the other compounds in this family, and could suggest either ligand-based redox events [the tris(alkoxyphenyl)methane caps are oxidatively sensitive[15]] or access to unique structures that afford improved electronic coupling (vide infra).

***O,N,O*-Ligated Trimetallic Complexes Containing a μ_3-Oxide or μ_3-Hydroxide.** In three of the four trinuclear complexes reported above, metalation using metal chlorides afforded compounds in which a chloride coordinates to each metal center in the complex. In an effort to use the steric constraints of the ligand to enforce an open-coordination site

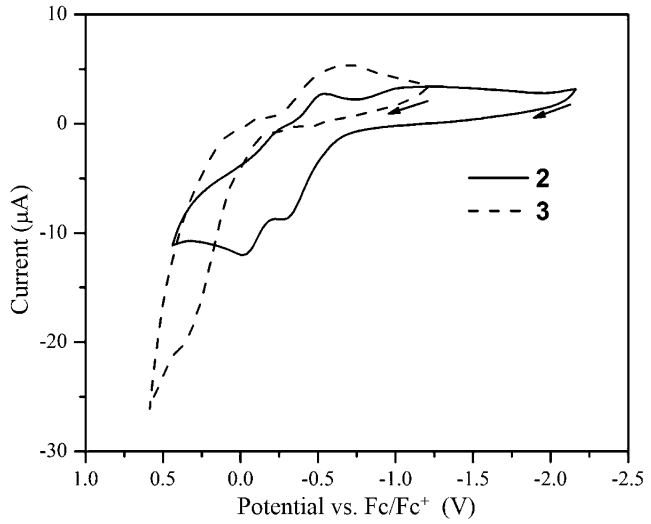

Figure 5. Cyclic voltammograms for **2** and **3** in MeCN at a scan rate of 150 mV/s. 0.1 M $TBAPF_6$ used as supporting electrolyte. Working electrode: 1 mm Pt button. Auxiliary electrode: Pt wire. Reference electrode: $Ag/AgNO_3$ in MeCN.

oriented toward the internal cavity, we explored other metal ion sources and, specifically, the hexamethyldisilazide and trifluoromethanesulfonate ($^-$OTf) salts. For the former, products were ill-defined and difficult to isolate and characterize. In the course of our studies using iron(II) and cobalt(II) triflates (triflate = trifluoromethanesulfonate) as metal precursors, we synthesized two complexes as the major product in which each pyridine dicarboxamide adopts an atypical *O,N,O*-coordination mode to each metal center.

Reaction of 3.3 equiv of KH with $H_6\mathbf{L}$ followed by addition of the bis(acetonitrile) adduct of either $Fe(OTf)_2$ or $Co(OTf)_2$ yielded the trinuclear *O,N,O*-coordinated compounds $[(Fe(MeCN))_3(\mu_3\text{-}O)\mathbf{L}H_5][OTf]_4$ (**5**) and $[Co_3(\mu\text{-}OH)(\mu_3\text{-}OH)(\mu\text{-}OTf)(OTf)(MeCN)\mathbf{L}H_6][OTf]_2$ (**6**), respectively. Both complexes are synthesized in good yield at 79% and 51% for the iron and cobalt species, respectively. Two aspects of the syntheses are worth noting: first, the optimized syntheses require half of the equivalents of KH as compared to the syntheses of **1**–**4**, and second, acetonitrile is an essential cosolvent in the reaction as the products are isolated in poor yield if this solvent is omitted. Independent of the intense infrared absorptions arising from the triflate anions in **5** and **6** (viz. 1028 and 637 cm^{-1}), there are other systematic differences between the IR spectra of **5** and **6**, and of **1**–**4**: the relative intensity for the absorptions at 1100 and 960 cm^{-1} are significantly reduced, and new intense features arise at 1631, 1556, 1233, 1203, and 1170 cm^{-1} in spectra of **5** and **6** (Figures S11 and S12, Supporting Information).

As alluded to above, each pyDCA arm coordinates to the metals in an *O,N,O*-fashion, and a μ_3-oxide bridge is installed within the center of the cluster in the structure of **5** (Figure 6). To adopt this unique coordination mode for pyDCA to iron, the donor arms rotate the appended carbonyl oxygen atoms toward the interior of the scaffold and dramatically alter the aspect ratio of the complex relative to the *N,N,N*-chelated compounds **1**–**4**. The distance between the central C atoms in each cap increases by ∼3.45 Å, and the pyridyl *N*-atoms move inward toward the internal cavity by ∼3.21 Å as compared to **1**. The coordination geometry around each iron atom is best described as distorted square pyramidal with O1, N2, O2, and

DOI: 10.1021/ic502873d
Inorg. Chem. 2015, 54, 2691–2704

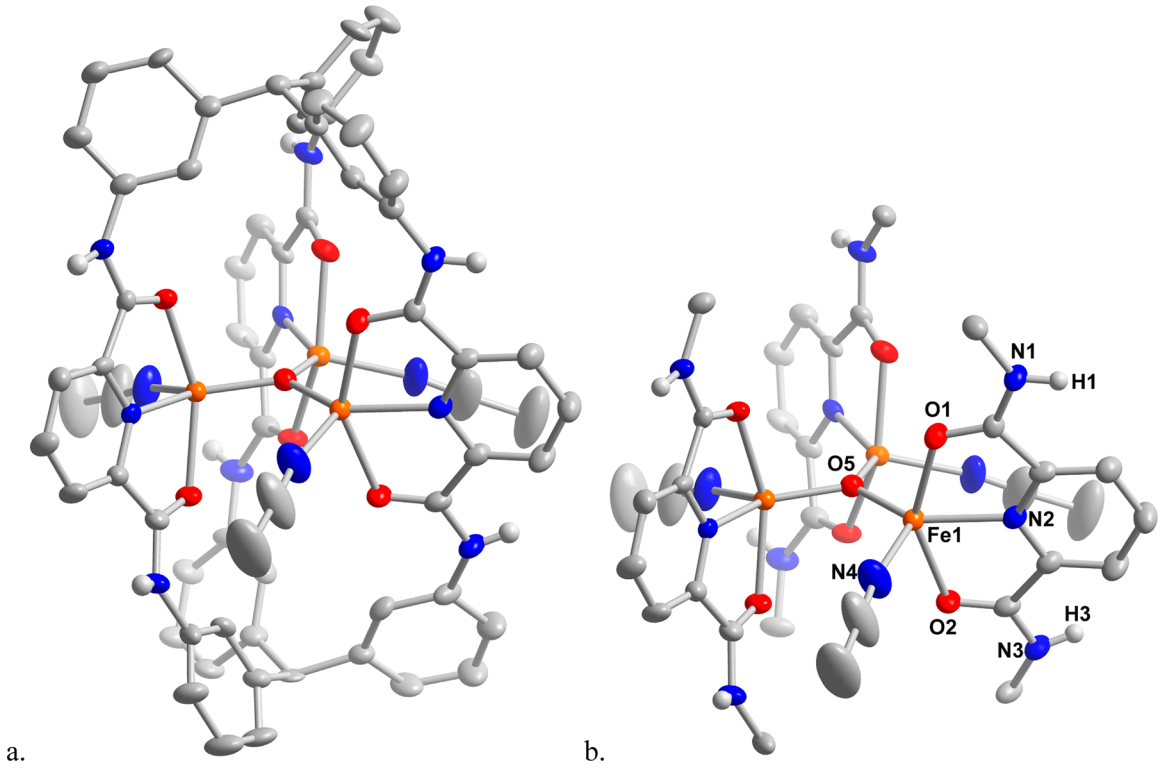

Figure 6. Solid state structure of **5** collected at 100 K (a) and cut away of the central cavity (b). C, H, N, O, and Fe atoms are represented as gray, light gray, blue, red, and orange ellipsoids (60%), respectively. All H atoms have been removed (except those on amide moieties which were freely refined) along with solvents of crystallization, four triflate anions, and the OEt and iPr substituents for clarity. Symmetry operations were used to generate equivalent atoms: $y - x$, $1 - x$, z; $1 - y$, $1 + x - y$, z.

O5 forming the basal plane and N4 of the coordinated MeCN occupying the axial position (τ = 0.19) and Fe1 held 0.616 Å out of the basal plane and shifted toward N4. The four outer-sphere triflate counteranions in the structure of **5** and the amide protons, which were refined freely, suggest that the complex is presumably tetracationic with the formula $[Fe_3(MeCN)_3(\mu_3\text{-}O)H_6\mathbf{L}]^{4+}$ and an oxo-bridged triiron(II) cluster housed within the ligand; however, this formulation is not congruent with all spectroscopic and magnetic data. The planarity observed for the $\{Fe_3O\}$ cluster in **5** is similar to that reported for other oxo-bridged triiron compounds,[16] whereas hydroxide bridged complexes are typically more pyramidalized. In addition, the Fe−O_{oxo} bond length of 1.8721(6) Å in **5** is comparable to ferrous pentanuclear helicates reported by Kawata[16a] (1.868 Å, 1.929 Å) and Oshio[16b] (1.882 Å, 1.904 Å) with all metal ions adopting a high-spin configuration. Two examples of mixed-valent, helicate polynuclear iron compounds are known in which monometallic pyDCA complexes with *N*,*N*,*N*-coordination nucleate the cluster.[17,18] One example shows clear shortening of the Fe−O_{oxo} bond length (av 1.856 Å) and loss of C_3 symmetry in the solid state[17] as expected with the incorporation of a ferric ion, whereas the other is assigned as an $Fe^{III}{}_2/Fe^{II}$ cluster and is C_3 symmetric in the solid state with longer Fe−O_{oxo} bonds (1.887 Å).[18] In **5**, however, the 3-fold crystallographic symmetry could allow one of the six amide protons to be disordered over either the upper or lower hemispheres of the structure, which in turn would afford a mixed valent species. At present, this argument seems the most reasonable considering the magnetic susceptibility data, the Mössbauer data, and the combustion analysis measurements (vide infra).

Given that oxo-bridged all-ferrous clusters are unusual, we first attempted to validate the protonation state of the amide N atoms by reacting **5** with MeOTf. ^{1}H NMR spectra of the organics isolated from acid hydrolysis of that product isolated after treating **5** with MeOTf were indistinguishable from that of $H_6\mathbf{L}$. To probe the oxidation state of the iron centers within the cluster, Mössbauer spectra and variable temperature magnetometry data were recorded on **5** (Figures 7 and 8, respectively). The zero-field Mössbauer spectrum measured at 80 K (Figure

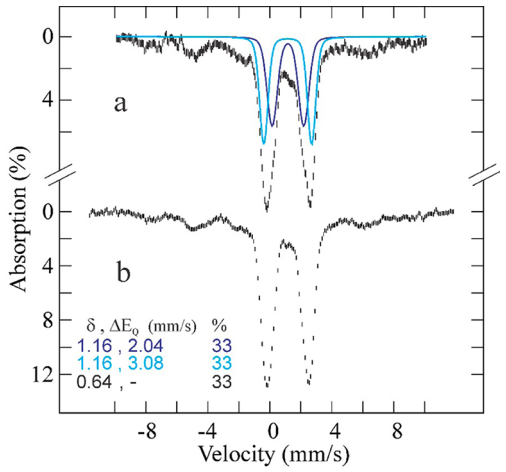

Figure 7. Zero-field, 80 K Mössbauer spectra of (a) a powder sample of **5** and (b) an acetonitrile solution of **5** synthesized with ^{57}Fe-enriched iron. The blue lines are quadrupole doublet simulations of the two components assigned to high-spin Fe^{II} centers with the parameters stated in the text.

DOI: 10.1021/ic502873d
Inorg. Chem. 2015, 54, 2691−2704

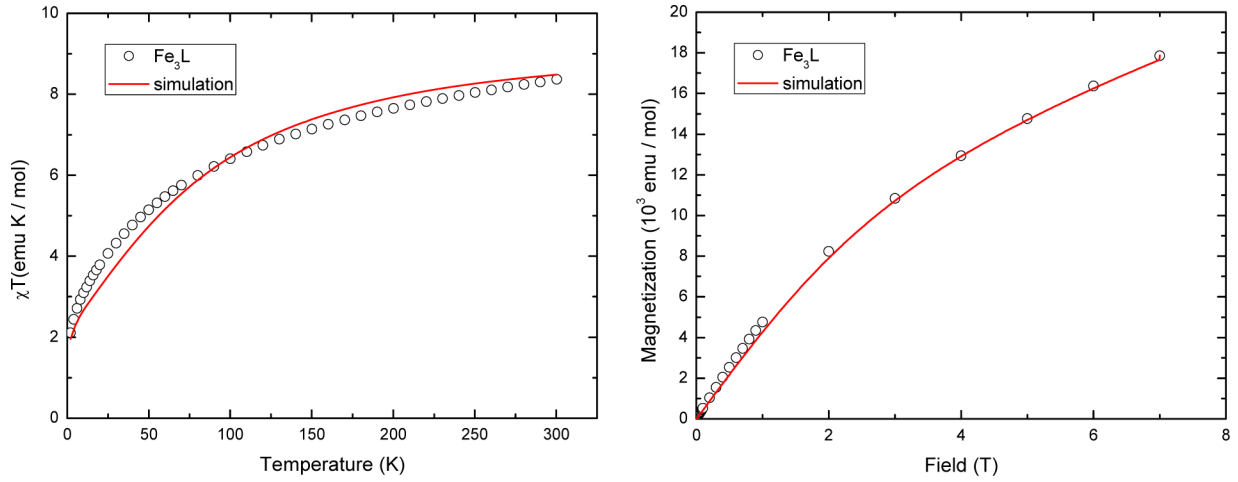

Figure 8. Variable temperature magnetometry in 10 mT (left) and field dependence of magnetization data collected at 5 K (right) of **5**.

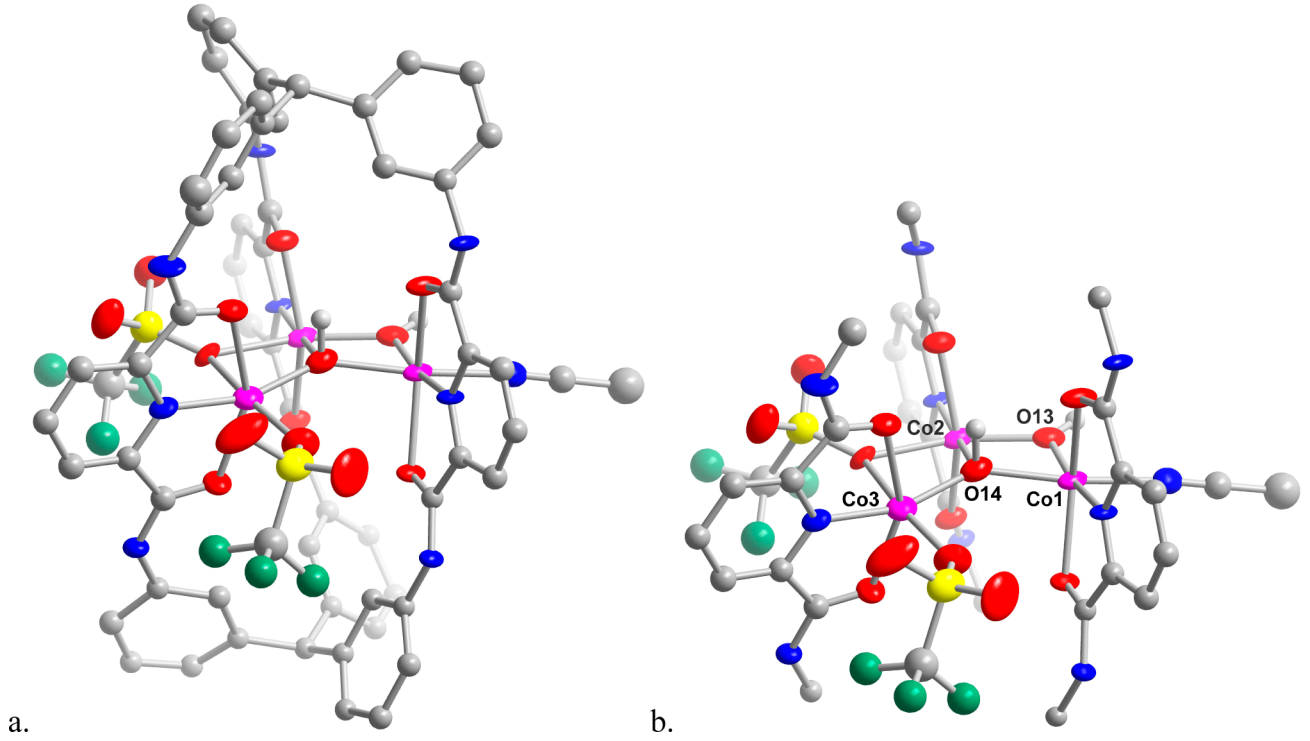

Figure 9. Solid state structure of **6** collected at 100 K (a) and cut away from the central cavity (b). C, H, N, O, S, F, and Co atoms are represented as gray, light gray, blue, red, yellow, teal, and pink ellipsoids (30%), respectively. All hydrogens have been removed (except calculated H positions on O13 and O14) along with solvents of crystallization, and two triflate anions for clarity.

7a) comprises a very broad doublet with parameters characteristic of high-spin Fe(II) and a magnetically split component accounting for roughly one-third of the total iron. Each peak of the doublet shows shoulders that clearly indicate that it is composed of at least two separate species. Indeed, it was successfully simulated with two symmetric doublets of equal intensities and parameters $\delta_1 = \delta_2 = 1.16$ mm/s, and $\Delta E_{Q1} = 2.04$ mm/s and $\Delta E_{Q2} = 3.08$ mm/s. The individual peaks are broad ($\Gamma_{1(FWHL)} = 0.83$ mm/s and $\Gamma_2 = 0.64$ mm/s) and are best fitted with Gaussian lines. These doublets are of equal intensity, and the simulated parameters are consistent with iron(II) centers in **5**. The δ and ΔE_Q values are comparable to those reported by Agapie and co-workers for the iron(II) centers in the mixed valent heterometallic oxo-triiron cluster[19] and in the oxo-triiron(II) complexes reported by Kawata[16a] and Oshio.[16b] Our values here are larger than those for the iron(II) centers in clusters reported by Betley and co-workers as might be expected, given the significant structural and electronic differences in their complexes as compared to **5** (e.g., absence of metal−metal interactions).[20] The magnetic component is a broad-line sextet centered on 0.64 mm/s that does not change shape with increasing temperature (up to 210 K). This observation is indicative of a half-integer spin system with a long spin−lattice relaxation time. The overall splitting and the isomer shift of the centroid are consistent with high-spin Fe^{III}. The line width and relaxation behavior may be attributed to magnetic ordering in the solid phase. In such a case, a solution spectrum should display different behavior as the paramagnets would be separated by solvent molecules. However, a sample of the complex synthesized from ^{57}Fe-enriched iron was

DOI: 10.1021/ic502873d
Inorg. Chem. 2015, 54, 2691−2704

subsequently dissolved in acetonitrile and yielded an identical spectrum with again a relative integration of the two signals of 2:1 (Figure 7b). This surprising invariability between solution and solid-state spectra could arise from the presence of insoluble nanoparticles of, for example, ferric oxide. We have however discarded this hypothesis based on other analyses (viz. elemental analyses and X-ray crystallography) that indicate that the complex is pure to 2% with the formula determined by X-ray crystallography. Additionally, the fact that the two Mössbauer components are in fixed, integer proportions support their assignment as different iron centers of the same multimeric complex, namely an $Fe^{II}Fe^{II}Fe^{III}$ mixed-valent trimer with localized valences.

On the basis of the oxidation states determined from the Mössbauer data, the spin system for **5** was defined with $S_1 = {}^5/_2$ and $S_2 = S_3 = 2$ corresponding to one iron(III) and two iron(II) centers in high spin configurations, respectively. From prior reports for (μ_3-oxo)triiron(II) and the mixed valent analogs,[16,21] EasySpin[22] simulations were constrained to single-ion anisotropy with the iron(III) and the iron(II) sites restricted to $|D| < 3\ cm^{-1}$ and $|D| < 30\ cm^{-1}$, respectively. In addition, the two iron(II) ions (S_2 and S_3) were treated as equivalent without including a rhombic anisotropy term to reduce the parameter space for the simulation and to avoid overparameterization. From our simulations, reasonable agreement to the temperature-dependent susceptibility data was only achieved for both J_{12} and $J_{13} < J_{23}$. Small negative value of D for iron(III) sites was required to model the low temperature regime of the susceptibility as well as the curvature of the field dependence of the magnetization. The best agreement, as shown by the solid lines in Figure 8, was obtained with values of $g_1 = 2$, $g_2 = g_3 = 2.03$, $D_1 = -1.45\ cm^{-1}$, $D_2 = D_3 = 3.47\ cm^{-1}$, and coupling constants of $J_{12} = J_{13} = -3.05\ cm^{-1}$ and $J_{23} = -6.35\ cm^{-1}$. Alternate values for S_1 of 2, ${}^3/_2$, and 1 were also used in these simulations, but a value of ${}^5/_2$ afforded the best agreement with the high temperature χT data.

In contrast to **5**, three unique cobalt centers are present in **6**, and each metal center is held in a pseudo-octahedral coordination environment (Figure 9). As observed in **5**, each pyDCA arm coordinates to a metal center through the amide carbonyl oxygen atoms and the pyridyl *N*-atom with a similar change in the aspect ratio of the complex as compared to **1**. Here, however, the observed electron density for the amide protons refines poorly, and the protons were therefore calculated. Further support of the assignment of each arm as protonated comes from the C═O and C—N bond distances, which fall within the range typical for O-bound neutral amides (O═C—NHR) as opposed to the deprotonated variant ($^-$O—C═NR).[23] We were unable to locate electron density corresponding to protons on the bridging O atom donors, and relied on the Co—O bond distances to assign the oxidation state of the metal ions and protonation state of the bridging ligands. The cationic complex is balanced by two outer-sphere triflate anions and contains two coordinated triflate ligands, for which the μ-1,1 bridging mode has not been reported previously. Therefore, the trimetallic core of **6** is likely tetracationic, suggesting that four possible assignments for the complex in which protonation of the bridging O atom donor is balanced by a Co^{II} instead of Co^{III} ion (e.g., $[Co^{II}{}_3(\mu_3\text{-OH})(\mu\text{-OH})]^{4+}$ and $[Co^{II}{}_2Co^{III}(\mu_3\text{-O})(\mu\text{-OH})]^{4+}$). First, the Co1—O13 and Co2—O13 bond distances are 1.930(5) Å and 1.958(5) Å and are within the range reported for high-spin Co^{II}—OH bonds.[24] Second, the distances between the three Co centers and the central O atom donor are 2.117(5) Å (Co1), 2.057(5) Å (Co2), and 1.940(5) Å (Co3), and the central O atom lies 0.4 Å below the Co_3 plane. These bond distances are slightly longer than the values reported for a hydroxide-bridged tricobalt cluster, and the hydroxide donor lies similarly out-of-plane of the three metal centers in that reported complex.[25] Finally, bond valence sum analysis supports the oxidation assignment of each metal center as Co^{II}, leading to an assignment of the bridging ligands as hydroxides (Table S4, Supporting Information).

The redox properties of the trinuclear clusters in **5** and **6** were investigated by cyclic voltammetry. Two broad, irreversible processes at −1.614 and −2.504 V are present in voltammograms of **5** as well as two pseudoreversible processes at 1.846 and 2.136 V. The broadness of the peaks is similar to our reported data for $[(FeCl_2)_3\mathbf{L}]^{3-}$, and agrees with the weak coupling between the metal centers from our simulations of the magnetometry data. A similar scenario was observed for **6** with the oxidative (2.003 and 1.683 V) and reductive (−1.227 and −1.597 V) events shifted to lower absolute values for the potentials (Figures S13−S14, Supporting Information).

The absence of reversible one-electron redox events in the data collected on both **5** and **6** was surprising given that the structural support offered by the macrobicyclic ligand was expected to provide stability to redox cycling. These results contrast the reversible couples observed for the heterometallic oxo-bridged triiron clusters reported by Herbert et al.[19] and the rich redox chemistry reported for the strongly interacting triiron clusters.[20] This difference can likely arise from the significantly weaker coupling between the metal centers in **5** as compared to the aforementioned ones. One possibility is that the perceived irreversibility could arise from ligand rearrangement upon reduction or oxidation of the cluster. Such structural changes are supported in our reactivity results (vide infra) in which treatment of N_3-ligated trimetallic compound with TMSOTf causes demetalation and rotation of one ligand arm from the *N,N,N*- to the *O,N,O*-arrangement.

We were interested in the source of oxide or hydroxide ligands in **5** and **6** as the reaction was carried out under anaerobic and anhydrous conditions. The isolated yields of both **5** and **6** suggest that neither ligand decomposition nor trace contaminants in the reagents is the source of these O atoms. Organic products consistent with solvent deoxygenation[26] were not observed by GC in the reaction headspace during the synthesis of **5**. The most likely candidate remains adventitious water, possibly from one of the reagents, solvents, and/or the glass surface. We attempted to synthesize **5** in the absence of KH, but this route was unsuccessful. Solvent, specifically acetonitrile, is the probable proton source because addition of acetonitrile to solutions of $\mathbf{L}^{6-}$ regenerates the free-base ligand. Moreover, the products are neither isolated nor observed from reactions in which acetonitrile is omitted. Access to *N,N,N*- versus *O,N,O*-coordination modes here could be determined by the ease of reprotonation and the size of the counteranion as compared to the internal cavity; that is, the smaller chloride is accommodated within the cavity whereas triflate is not, and the complex rearranges to generate coordinatively saturated metal centers. The effect of protonation state of the amide N atoms and the resultant effect on metal binding and the initial coordination mode are currently being explored to provide insights into the design of complexes with dynamic stimuli-driven structural properties. By way of a preliminary attempt to probe such chemical stimuli to effect

DOI: 10.1021/ic502873d
Inorg. Chem. 2015, 54, 2691−2704

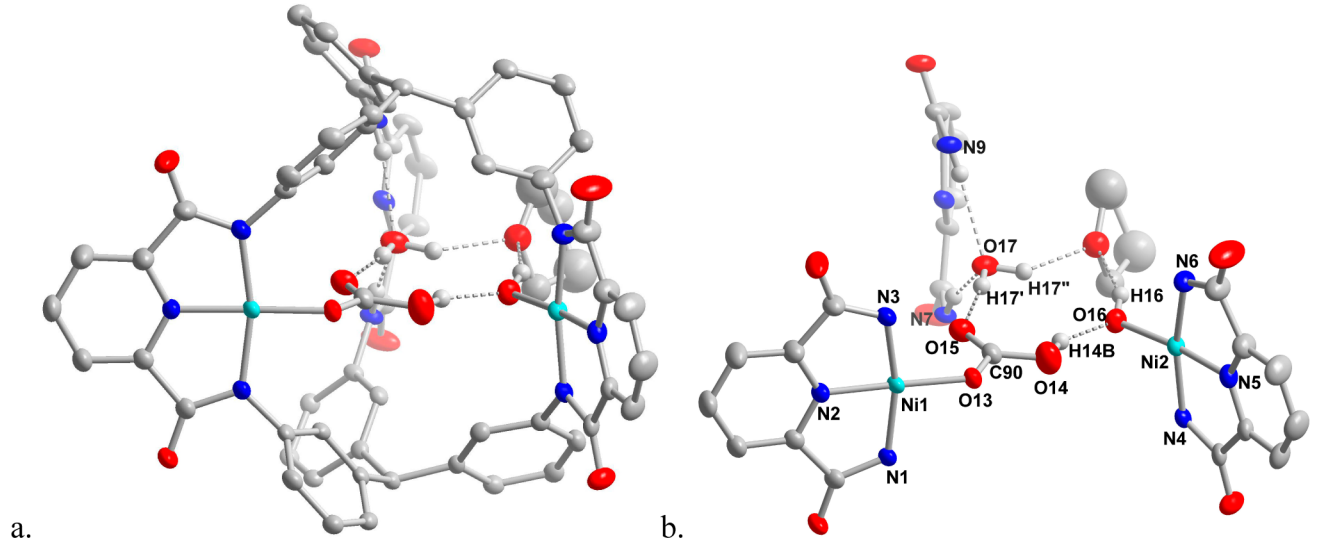

Figure 10. Solid state structure of **7** collected at 100 K (a) and cut away of the central cavity (b). C, H, N, O, and Ni represented as gray, light gray, blue, red, and aqua ellipsoids (60%), respectively. All H atoms have been removed except those which constitute the hydrogen bonding network in the cavity along with solvents of crystallization, three tetraethylammonium cations, one triflate anion, and the OEt and iPr substituents.

structural changes, we were intrigued as to whether the two complex types (i.e., *N,N,N* vs *O,N,O*) could be interconverted. Our first hypothesis was that halide abstraction from **2** would lead to coordinatively unsaturated metal centers frustrated by the steric constraints imposed by the ligand, and ultimately result in complex rearrangement. Preliminary work in which **2** is treated with 3 equiv of Me_3SiOTf yields a dimetallic complex, albeit in poor yield, for which the coordination mode changes from *N,N,N* to *O,N,O* for the two retained iron centers (Figure S16, Supporting Information). This preliminary result agrees with the proposed synergy between the electronic and steric effects in these complexes.

Preliminary Studies on O Atom Transfer Reactivity of 2. The ability of **2** to act as an oxygen atom transfer agent was probed using iodosobenzene as the O atom source and triphenylphosphine as the substrate. Although the size of the internal cavity would not accommodate PPh_3, its extensive use in O atom transfer studies and the flexibility of the ligand arms led to this choice of substrate. A series of conditions were surveyed in which the ratio of **2**:PPh_3:PhIO was varied, and we observed only Ph_3PO and no unreacted starting phosphine in reactions with the ratios of 1:1:3, 1:2:4, and 1:3:5; control reactions of PhIO with PPh_3 under similar conditions did not yield Ph_3PO (Figures S19−20 Supporting Information). Reactions with fewer equivalents of PhIO, such as 1:1:2 and 1:1:1, showed incomplete substrate oxidation with both Ph_3PO and PPh_3 present in the NMR sample. The number of equivalents of PhIO required to effect complete oxidation of triphenylphosphine suggests a possible activation step where **2** accepts an O atom from iodosobenzene, followed by structural rearrangements to afford the reactive O atom transfer complex. Such a rearrangement could traverse compounds in which *O,N,O*- or *N,N,O*-coordination modes are observed as the complex collapses to an oxo-centered trinuclear cluster. To probe whether O atom incorporation in **2** leads to other ligand coordination modes, we reacted **2** with iodosobenzene in the absence of substrates, but we were unable to isolate crystalline products from the reaction mixture, and the characteristic changes to the IR spectrum for *O,N,O*-coordination were not observed. Using a similar procedure as for Ph_3P oxidation, we evaluated O atom transfer by **2** from PhIO to styrene; however, we observed only styrene and not expected oxidation products in the product mixtures by gas-chromatography (data not shown). These results suggest a limit for the O atom transfer reactivity of the product of **2** and iodosobenzene, although steric effects cannot be excluded here. Ongoing work aims to define the substrate scope both in terms of sterics and electronic factors as well as the mechanism of O atom transfer.

Incorporation of Hydrogen Bonding Networks in Dimetalated Complexes. Prior reports on nickel(II) and copper(II) pyDCA complexes used hydroxide sources instead of stronger bases to simultaneously metalate and install a hydroxide ligand on the resultant complex.[10a,d,j] These mononuclear compounds sequester carbon dioxide reversibly (nickel)[10a−c] and support reactive metal−oxygen species (copper).[10e−h,j] In light of these types of reactivity, we pursued a similar synthetic approach using H_6**L** to define the interactions between the metal-hydroxides within the internal cavity. As a first step toward synthesizing these types of complexes, we aimed to test whether alkylammonium hydroxides were competent for deprotonation of the ligand and subsequent metalation using either copper or nickel triflate. Therefore, these reactions were performed on the benchtop, and we anticipated carbonate or bicarbonate complexes resulting from sequestration of atmospheric CO_2 based on reports by others on the monometallic pyDCA complexes.

Reaction of H_6**L** with 3 equiv of either $Ni(OTf)_2$ or $Cu(OTf)_2$ followed by excess tetraethylammonium hydroxide as a methanolic solution in the presence of ambient atmosphere led to an immediate color change from pale green or yellow to dark red or dark green, respectively, and ultimately afforded $[Et_4N]_2[Ni(OCOOH)Ni(OH)H_2L]$ (**7**) or $[Et_4N]_2[Cu_3(\mu\text{-}\eta^1{:}\eta^2\text{-}OCOO)(\mu\text{-}OH)(OH)H_2L]$ (**9**) in good yield. Even though we were able to isolate the dinickel complex from the product mixture (Figure S17, Supporting Information), the reaction residues were quickly washed with aqueous sodium or potassium hydroxide solutions to remove the $[Et_4N][OTf]$ byproduct. Surprisingly, this seemingly nominal difference between alkali cations afforded unique products for both the Ni and Cu complex syntheses. Reaction of 3 equiv of $Ni(OTf)_2$

DOI: 10.1021/ic502873d
Inorg. Chem. 2015, 54, 2691−2704

and 9 equiv of Et_4NOH followed by a KOH wash reproducibly afforded **7** whereas a NaOH wash led to mixtures from which we were able to isolate a sodium inclusion complex, $[Et_4N]_2[Ni_2(\eta^1\text{-}OH)(\mu\text{-}\eta^1\text{:}\eta^2\text{-}CO_3)LH_2Na(THF)]$, in poor yield (Figure S18, Supporting Information).

X-ray quality crystals of **7** were isolated as red blocks from diffusions of diethyl ether into tetrahydrofuran solutions of the reaction mixture (Figure 10). As expected, the complex incorporates a bicarbonate ligand on one nickel center; however, we were surprised that the ligand here is only partially metalated, with two nickel cations held within an *N*,*N*,*N* chelate, and the third pyDCA arm remains unmetalated. The bicarbonate ligand is hydrogen bonded to the hydroxide ligand on the neighboring nickel ion as well as to a water molecule within the central cavity. Second coordination sphere hydrogen bonding interactions have been previously incorporated into monometallic copper pyDCA complexes. In these systems, hydrogen bond donors were appended to the pyDCA amide groups and interact with the terminal chloride coordinated to the metal center.[27] Unlike these monometallic complexes, hydrogen bonding interactions in **7** result from partial metalation of the cryptate, incorporates solvent molecules, and extends throughout the internal cavity, beginning with the metal-bound bicarbonate and hydroxide and terminating with the amide protons H9 and H7 on the unmetalated pyDCA arm. We were unable to locate the bicarbonate proton in the difference map, but it was instead calculated on O14 on the basis of the following observations. First, the C90−O bond distances are comparable to those reported for the bicarbonatonickel(II) pyDCA compound reported by Holm and co-workers, and the C90−O14 distance is longer than that for C90−O15.[10a] Second, the protons on the water molecule within the cavity and on the hydroxide ligand were located and freely refined, and the orientations of these H atoms and the distance between O14 and O18 are consistent with the presence of a hydrogen bond. Third, charge balance considerations favor a bicarbonate donor. Although there are numerous prior examples of polynuclear nickel(II) complexes in which either CO_3^{2-} or HCO_3^- coordinate in a bridging fashion,[28] this complex represents a unique case in which both a terminal Ni−OH and an Ni−OC_2OH coexist in the same complex. It is evident that the ligand precludes a bridging coordination mode for the bicarbonate donor as the cryptand enforces a limited range of possible metal−metal distances in the *N*,*N*,*N*-coordination mode.

A number of mononuclear hydroxide complexes sequester carbon dioxide as bicarbonate or carbonate with subsequent release of CO_2 either by sparging with an inert gas or by degassing a solution of the bicarbonate complex.[10a−c,28h,29] These compounds parallel the reactivity of carbonic anhydrase, in which a terminal hydroxide bound to the active site Zn^{II} captures CO_2, which then dissociates as bicarbonate.[11] We therefore investigated if release of CO_2 could be accomplished from **7**. To our surprise, sparging solutions of **7** with N_2, repeated cycles of freeze−pump−thaw, or heating a solid sample under dynamic vacuum (<10 mT) resulted in no change in the ^1H NMR or IR spectra (Figure S21, Supporting Information). Evidently then, CO_2 release in our multimetallic system is more energetically demanding than the comparable monometallic complexes, and we attribute this difference to the additional energy required to break the hydrogen bonding network. This result provides strong evidence that incorporating similar arrays in extended solids or molecular systems will lead to highly effective CO_2 capture reagents.

The bicarbonate ligand could arise from reaction of Et_4NOH with carbon dioxide prior to complex formation. As noted above, however, we suspected that metalation under conditions used to synthesize **7** initially affords a complex containing either one or two nickel-hydroxide centers, in which a Ni^{II}−OH moiety rapidly sequesters an equivalent of atmospheric carbon dioxide. Then, the steric constraints of the internal cavity, hydrogen bonding interactions, or other electrostatic effects would disfavor capture of a second equivalent of CO_2 to install a second bicarbonate donor. To test this hypothesis, the di(hydroxonickel(II)) complex **8** was synthesized using a procedure analogous to that for **7** except that the reaction was sparged with nitrogen prior to adding Et_4NOH and maintained under an inert atmosphere thereafter. ESI(−)/MS data collected on solutions of **8** contain an isotopic pattern consistent with the expected $[C_{89}H_{99}N_9Ni_2O_{14}]^{2-}$ at 817.8005 *m*/*z* as well as an ion envelope of much lower intensity corresponding to **7**, which could be present as a minor product or arise from reaction with adventitious carbon dioxide during MS data collection (Figure S22, Supporting Information). We were unable to remove the EtN_4OTf byproduct from the reaction for satisfactory combustion analysis, and further studies were carried out on the complex as-synthesized. To avoid exposure to CO_2, NMR spectra were recorded on a rigorously dried sample of **8** in anhydrous solvent. From NMR spectra of both **7** and **8** under air-free and anhydrous conditions in d_8-THF, it was readily apparent that, whereas spectra of **7** in solvents containing trace water were well-resolved, those collected in anhydrous solvent indicated that multiple species are present upon exclusion of water. We postulated that the complex might lock into multiple conformations of comparable energies in the absence of water, likely enforced by the hydrogen bonding interactions on the interior of the compound. Thus, exposure of an anhydrous sample of **7** in $CDCl_3$ to air for a short period of time results in broadening of the spectrum and ultimately reversion to spectra recorded in as-received $CDCl_3$. Although broad resonances are present in spectra of the di(NiOH) complex **8**, we observe resonances in the range −3.5 to −5 ppm, which are typical for terminal nickel-hydroxides.[10a,d,30] In support of our hypothesis that CO_2 can be sequestered by a transient di(NiOH) complex in the synthesis of the bicarbonate-containing complex **7**, exposure of an anhydrous sample of the di(NiOH) complex **8** in THF to CO_2 for 1 h results in changes in the spectrum that are consistent with formation of **7** as well as free ligand (Supporting Information Figure S24). Similarly, exposure of a sample of the di(NiOH) complex **8** as a solid to air for 12 h afforded the bicarbonate complex **7**, albeit with a similar amount of the free ligand as determined by ^1H NMR spectra (Supporting Information Figure S25). As anticipated then, one of the terminal nickel-hydroxide sites within **8** is competent for CO_2 capture. This result also suggests that whereas the bicarbonate complex **7** is stable in wet NMR solvents, the di(NiOH) complex is more sensitive and undergoes demetalation more readily.

Demonstrating the generality of this synthetic approach to the dimetalated compounds, reaction of 3 equiv of copper(II) triflate with $H_6\mathbf{L}$ followed by excess Et_4NOH afforded $[Et_4N]_2[Cu_3(\mu\text{-}\eta^1\text{:}\eta^2\text{-}CO_3)(\mu\text{-}OH)(OH)\ H_2\mathbf{L}]$, **9**, in good yield (40%). The molecular structure of this copper complex is similar to that of the bicarbonate-containing compound **7** as

DOI: 10.1021/ic502873d
Inorg. Chem. 2015, 54, 2691−2704

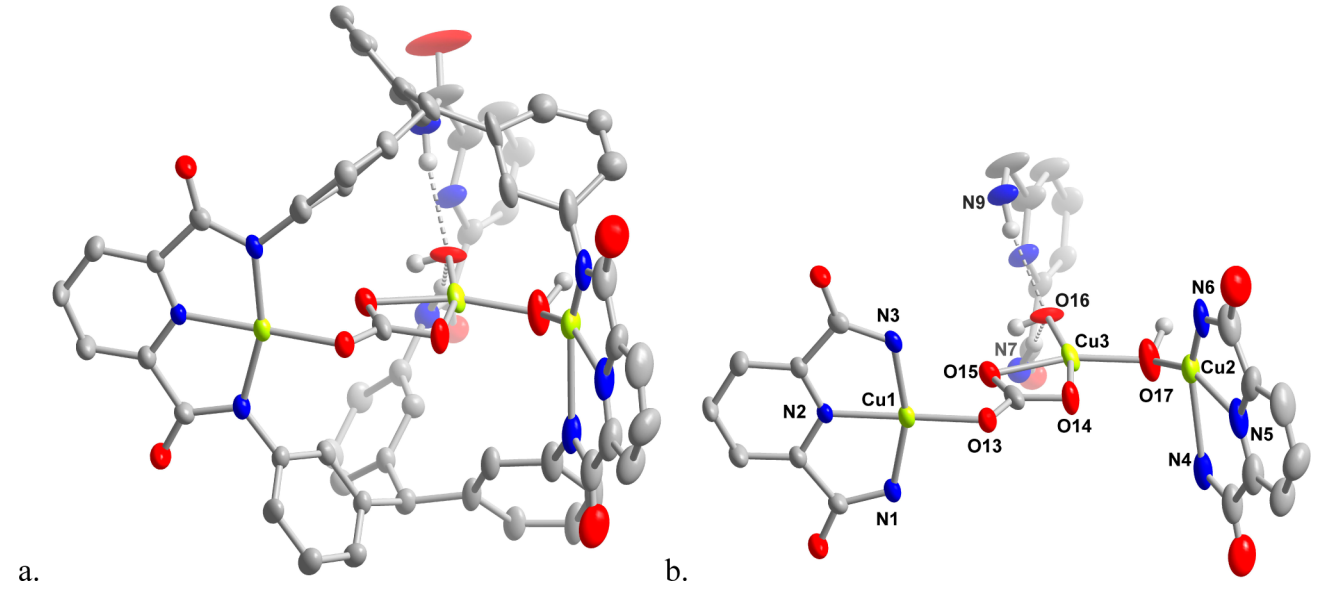

Figure 11. Solid state structure of **9** collected at 100 K (a) and cut away of the central cavity (b). C, H, N, O, and Cu atoms are represented as gray, light gray, blue, red, and yellow-green ellipsoids (30%), respectively. All hydrogens have been removed except amide and hydroxide hydrogens (all shown H positions are calculated) along with solvents of crystallization, two tetraethylammonium cations, and the OEt and iPr substituents.

there are two Cu^{2+} ions coordinated in an *N,N,N*-chelate of two arms of the cryptand (Figure 11). However, a third metal ion is present within the internal cavity of **9** and is held within a distorted square planar coordination environment comprising the hydroxide ligated to Cu2, η^2-coordination of the carbonate on Cu1, and an additional hydroxide donor. This structure was not of the appropriate quality to refine the positions of H atoms on O16, O17, N7, or N9, so these positions were calculated and included on the basis of charge balance and the observed bond lengths. In particular, the Cu2−O17 distance is 1.971(2) Å, the Cu3−O17 distance is 1.852(2) Å, and the Cu3−O16 distance is 1.9773(17) Å. Cu−O bonds lengths (∼1.90 Å) in the hydroxo-bridged copper-pyDCA complex reported by Tolman[10j] are comparable to those of **9**. Elongation of the Cu2−O17 (1.971(2) Å) and Cu3−O16 (1.9773(17) Å) is observed; however, only 73% occupancy of Cu2 is observed as this metal center is disordered over two positions in the structure solution. Square planar copper(II) complexes for which a carbonate coordinates in an η^2 manner have only been reported previously for N atom donor ligands.[28b,31] The subtle differences that generate the trimetallic species **9** as compared with the dimetallic **7** are unclear, but the greater basicity of the terminal hydroxides of copper-pyDCA complexes as compared to nickel-pyDCA compounds may favor coordination of the excess Cu(II) in solution.

We initially expected from reports on mono-pyDCA complexes that substituting Et_4NOH for stronger bases would yield complexes with each doubly deprotonated pyDCA arm coordinating a metal center. For both copper(II) and nickel(II), however, only two of the three pyDCA donor arms are metalated. One hypothesis is that specificity for partial metalation arises from a balance between the increasing pK_a values for each subsequent amide proton and that of water.[31d] In particular for these hydroxide-decorated complexes, an electrostatic component could contribute to the partial metalation as each anionic hydroxide donor is oriented toward the internal cavity, thereby disfavoring both deprotonation and approach of weaker bases, and the association of countercations with the partially metalated complexes could contribute a steric effect. Interestingly, the ability to use solvent and choice of base to target these dimetallic complexes is analogous to recent reports by Powers et al. in which solvent choice biases the metalation of a hexadentate ligand to afford either trinuclear or dinuclear complexes. Such subtle strategies may therefore be common approaches to tuning the nuclearity of metal clusters templated by multidentate ligands.[32]

OUTLOOK

The macrobicyclic cryptand, H_6**L**, offers an unusual utilitarian platform to assemble multimetallic compounds as the donor atom types can be readily tuned, hydrogen bonding interactions incorporated, and the extent of metalation controlled. The results presented here point to an ability to rationally modulate all of these parameters using base strength, choice of metal precursor, and solvent identity. Initial results point to clear divergence from reaction outcomes seen for monometallic complexes with different reactivity patterns and access to unique structural motifs.

EXPERIMENTAL SECTION

General Considerations. Reactions necessitating dry, air free conditions were performed using standard Schlenk techniques or in an Innovative Technologies glovebox. Anhydrous solvents were extracted from an Innovative Technologies solvent purification system. Anhydrous divalent metal halides were purchased from either Strem Chemical or Sigma-Aldrich and dried first with $SOCl_2$ and then heated under vacuum. Both potassium and sodium hexamethyldisilazide were purchased from Sigma-Aldrich and used as received. Potassium hydride was purchased from Sigma-Aldrich and was rinsed with anhydrous hexanes prior to use. 18-Crown-6 was gently heated under vacuum prior to storage in the glovebox. NMR spectra were recorded on either a 500 MHz Inova or 300 MHz Mercury spectrophotometer with the spectra referenced to the residual protonated solvent signal, 7.27 ppm for $CDCl_3$ and 3.58 for THF-d_8. Deuterated solvents were purchased from Cambridge Isotope Laboratories and when necessary dried according to standard procedures. Infrared spectra were recorded as solids on a Bruker Vertex 80v FTIR using a Pike GladiATR stage, or were collected under air-free conditions on a Bruker Alpha FTIR equipped with a diamond ATR stage inside the glovebox. Cyclic

DOI: 10.1021/ic502873d
Inorg. Chem. 2015, 54, 2691−2704

voltammetry was performed under a nitrogen atmosphere using a standard three electrode setup. Electrodes were purchased from either BASi, Inc., or CH Instruments, Inc. Potential sweeps were controlled by a Princeton Applied Research Versastat II potentiostat. Elemental analyses were performed by Complete Analysis Laboratories, Inc. (Parsippany, NJ). The bis(acetonitrile) adducts of the metal trifluoromethanesulfonate salts were synthesized by reacting a slurry of metal dihalide in anhydrous air-free acetonitrile with 2 equiv of trimethylsilyltrifluoromethanesulfonate (Me_3SiOTf) for 2 h, and the products recrystallized by diffusion of diethyl ether into a saturated MeCN solution. Coordinated solvent molecules were removed by heating under vacuum. Tetraethylammonium hydroxide solution (1.5 M in methanol) was purchased from Sigma-Aldrich. The solution was transferred from the reagent bottle into a storage flask by cannula and stored under an inert atmosphere, and aliquots for reactions were removed using a syringe and under a positive pressure of dinitrogen. Mass spectra were collected by direct injection using either negative or position mode and an appropriate anhydrous solvent. Samples were input into the instrument using gastight syringes and a syringe pump via HPLC tubing. The tubing was prerinsed with anhydrous solvent also in a gastight syringe before introduction of the sample.

X-ray Crystallography. X-ray intensity data were collected at 100 K on a Bruker DUO diffractometer using Mo Kα radiation (λ = 0.710 73 Å) or Cu Kα radiation (λ = 1.541 78 Å) from an ImuS power source, and an APEXII CCD area detector. Raw data frames were read by the SAINT3 program and integrated using 3D profiling algorithms. The resulting data were reduced to produce *hkl* reflections and their intensities and estimated standard deviations. The data were corrected for Lorentz and polarization effects, and numerical absorption corrections were applied on the basis of indexed and measured faces. The structures were solved and refined in SHELXTL6.1, using full matrix least-squares refinement. The non-H atoms were refined with anisotropic thermal parameters, and all of the H atoms were calculated in idealized positions and refined riding on their parent atoms unless otherwise stated. Details specific to data refinement and structure solutions for each compound are reported in the Supporting Information.

[K(18-Crown-6)]$_2$[K(Cu^{II}Cl)$_3$L] (1). A portion of H_6L (200 mg, 0.134 mmol) was dissolved in THF (~8 mL) and cooled to −78 °C. A solution of KHMDS (177 mg, 0.887 mmol) was made in THF (2 mL) and also cooled to −78 °C. The KHMDS solution was then added dropwise to the solution of H_6L causing an immediate change from a colorless solution to yellow. The reaction was stirred for approximately 30−60 min followed by the addition of a solution of 18-crown-6 (107 mg, 0.403 mmol) in 0.5 mL of THF. $CuCl_2$ (60 mg, 0.44 mmol) was then added to the reaction. The reaction immediately took on a deep green color. The reaction was warmed to room temperature and stirred overnight. The reaction was then filtered, and the solvents were removed under reduced pressure. The residue was taken up in a minimum of THF (2 mL) and the complex precipitated with diethyl ether (15 mL). The residue was collected by filtration, suspended, and stirred in diethyl ether for 8 h, and recollected by filtration to afford a green powder (127 mg, 39% yield). X-ray quality crystals were grown by slow diffusion of dimethoxyethane into a tetrahydrofuran solution. IR: 2866 (m), 1585 (s), 1453 (s), 1208 (s), 1102 (s), 898 (m) cm^{-1}. HRMS-ESI(−): m/z 909.1862, calcd for $[C_{89}H_{95}N_9O_{12}Cu^{II}{}_3Cl_3K]^{2-}$ 909.1845. Anal. Calcd for $C_{113}H_{143}Cl_3Cu_3K_3N_9O_{24}$: C, 55.95; H, 5.94; N, 5.20; Cu, 7.86; Cl, 4.38; K 4.84. Found: C, 55.98; H, 6.01; N, 5.04; Cu, 8.02; Cl, 4.28; K, 4.53.

[K(18-Crown-6)]$_2$[K(Fe^{II}Cl)$_3$L] (2). This compound was synthesized using the method described for **1** with the following exceptions. Addition of $FeCl_2$ to the ligand deprotonated with 6.6 equiv of KH afforded a red/brown reaction mixture, and the crude product was recrystallized from diffusion of diethyl ether into a concentrated solution of THF yielding the desired product as a red/brown powder in 78% yield. IR: 2866 (m), 1575 (s), 1456 (s), 1351 (s) 1103 (s) cm^{-1}. Evans' method (CD_3CN): μ_{eff} = 7.83(4). HRMS-ESI(−): m/z 897.6907, calcd for $[C_{89}H_{95}N_9O_{12}Fe^{II}{}_3Cl_3K]^{2-}$ 897.6931. Anal. Calcd for $C_{113}H_{143}Cl_3Fe_3K_3N_9O_{24}$: C, 56.49; H, 6.00; N, 5.25. Found: C, 56.32; H, 6.35; N, 5.25.

Reaction of Ph_3P with Iodosobenzene and 2. A portion of **2** (20 mg, 0.0083 mmol) was dissolved in MeCN (7 mL), and triphenylphosphine (1, 2, or 3 equiv to **2**) was added. Then, iodosobenzene (1, 2, or 3 equiv to **2**) was added to the reaction, and the mixture stirred at room temperature for 6 h. The solvent was removed under reduced pressure and the residue redissolved with vigorous stirring in deuterated benzene. The sample was filtered through Celite, and ^{31}P NMR spectra were collected using 85% H_3PO_4 as the reference. The ratio of the integrands for peaks corresponding to triphenylphosphine and triphenylphosphineoxide were determined.

[K(18-Crown-6)]$_2$[K(Co^{II}Cl)$_3$L] (3). The tricobalt complex was synthesized using the method described for **2** with the following observed differences. Addition of $CoCl_2$ to the deprotonated ligand afforded a green reaction mixture, and the crude product was recrystallized from diffusion of diethyl ether into a concentrated solution of THF yielding the desired product as a green microcrystalline powder in 92% yield. IR: 2865 (m), 1573 (s), 1453 (s), 1351 (s) 1103 (s) cm^{-1}. Evans method (CD_3CN): μ_{eff} = 6.81(3) μ_B. HRMS-ESI(−): m/z 902.1948, calcd for $(C_{89}H_{95}N_9O_{12}Co^{II}{}_3Cl_3K)^{2-}$ 902.1907. Anal. Calcd for $C_{113}H_{143}Cl_3Co_3K_3N_9O_{24}$: C, 56.27; H, 5.98; N, 5.23. Found: C, 56.12; H, 5.88; N, 5.25.

[18-Crown-6-K][(Ni(THF))$_2$(NiCl)L] (4). A sample of H_6L (38 mg, 0.026 mmol) was dissolved in THF (12 mL), and KH (6.7 mg, 0.17 mmol) was added to the solution. The reaction was stirred for 1 h and then filtered through Celite. 18-Crown-6 (7 mg, 0.03 mmol) was then added to the yellow solution followed by $NiCl_2$·1.5THF (20 mg, 0.084 mmol). The reaction was stirred for 48 h at 50 °C to afford a red-brown slurry, which was then filtered through Celite and the filtrate dried under vacuum. The brown residue was recrystallized by diffusion of diethyl ether into a THF solution of the residue affording brown crystals. The crystals were dried for 4 h at 50 °C under reduced pressure (34 mg, 62% yield). IR: 2961 (m), 1630 (s), 1590 (m), 1449 (s), 1028 (s), 901 (m) cm^{-1}. HRMS-ESI(−): m/z 873.7324, calcd. for $[C_{89}H_{97}N_9Cl_2Ni_3O_{13}]^{2-}$ 873.7311. Anal. Calcd for $C_{109}H_{135}N_9Ni_3O_{20}$: C, 61.12; H, 6.35; N, 5.89. Found: C, 61.01; H, 6.37; N, 5.84.

[(Fe(MeCN))$_3$(μ_3-O)LH$_5$][OTf]$_4$ (5). A 100 mL round-bottom flask was charged with H_6L (0.882 g, 0.592 mmol) and THF (40 mL). A 50% dispersion of KH (0.157 g, 0.195 mmol) was added at room temperature causing the solution to change from colorless to yellow with the release of hydrogen gas. The reaction was stirred for 1 h at ambient temperature after which $Fe(OTf)_2$·2MeCN (0.853 g, 1.95 mmol) was added in one portion. The dark intensely colored reaction mixture was stirred for 12 h after which the solvent was removed under reduced pressure. The residue was dissolved in a minimum of acetonitrile (10 mL) and the solution filtered through Celite. Toluene diffusion into the acetonitrile solution over the course of 2 days resulted in crystallization of KOTf (263 mg), which was removed by filtration. 18-Crown-6 (150 mg, 0.568 mmol) was added to the solution, which was then diluted with toluene and placed in a freezer at −40 °C for 2 h. The flocculent, purple precipitate was collected by filtration, redissolved in a minimum of MeCN (8 mL), and diffusion of toluene into this solution afforded the target complex as black crystals (1.111 g, 79%). IR: 2964 (m), 1631 (s), 1556 (s), 1456 (s), 1209 (s) 1028 (s), 636 (s) cm^{-1}. Anal. Calcd for $C_{99}H_{110}F_{12}Fe_3N_{12}O_{25}S_4$: C, 49.71; H, 4.64; N, 7.03. Found: C, 49.72; H, 4.72; N, 6.92.

Reaction of 5 with Methyl Trifluoromethylsulfonate. Complex **5** (54 mg, 0.023 mmol) was dissolved in THF (8 mL), and methyl trifluoromethanesulfonate (2.8 μL, 0.025 mmol) was added. The reaction was stirred overnight after which the solvent was removed under reduced pressure to yield a tacky black solid. This residue was removed from the anaerobic chamber, redissolved in dichloromethane (8 mL), and hydrolyzed and demetalated by washing with an aqueous solution containing a large excess of Na_2EDTA (8 mL). The organic layer was separated, dried with magnesium sulfate, and the solvent removed under reduced pressure yielding 25 mg of off-white powder. NMR spectra collected on the residue in $CDCl_3$ indicated that the isolated compound was the nonalkylated, free ligand H_6L. Isolated mass corresponds to 46% recovered yield.

[Co$_3$(μ-OH)(μ_3-OH)(μ-OTf)(OTf)LH$_6$][OTf]$_2$ (6). H_6L (203 mg, 0.136 mmol) was dissolved in THF (~10 mL), and KH (18 mg, 0.43

DOI: 10.1021/ic502873d
Inorg. Chem. 2015, 54, 2691−2704

mmol) was added in one portion. Once effervescence ceased, $Co(O_3SCF_3)_2$·2MeCN (190 mg, 0.432 mmol) was added to the pale yellow reaction mixture, which immediately became a mahogany colored mixture. The reaction was stirred overnight, and then was filtered, and the solvent removed from the filtrate under reduced pressure. The residue was dissolved in a minimum of MeCN and toluene diffused into the solution to afford colorless crystals of KOTf, which were separated from the mother liquor by filtration. This method of removing KOTf from the crude product was repeated a second time. 18-Crown-6 (10 mg, 0.38 mmol) was then added to the mother liquor, followed by toluene. The mixture was filtered and the desired product isolated as a green solid. Storing the filtrate at −32 °C yielded a second crop of the product. The isolated compound was dried under reduced pressure yielding a green solid (162 mg, 51%). IR: 2964 (m), 1633 (s), 1556 (s), 1461 (s), 1209 (s) 1028 (s), 634 (s) cm^{-1}. Evans method (CD_3CN): μ_{eff} = 7.54(3) μ_B. Anal. Calcd for $C_{95}H_{106}F_{12}Co_3N_{10}O_{26}S_4$: C, 48.82; H, 4.57; N, 5.99. Found: C, 48.82; H, 4.39; N, 5.93.

$[Et_4N]_2[Ni(OCOOH)Ni(OH)H_2L]$ (7). Synthesis of the target complex was carried out on the benchtop and exposed to ambient air. To a solution of H_6**L** (51 mg, 0.034 mmol) in THF (10 mL) was added $Ni(OTf)_2$·2MeCN (45 mg, 0.10 mmol). Tetraethylammonium hydroxide in methanol (1.5 M, 0.210 mL, 0.316 mmol) was added dropwise to the pale green reaction mixture. The reaction flask was capped with a septum, and the resulting red solution was stirred overnight at room temperature and subsequently filtered through Celite, and the filtrate dried under reduced pressure. The red solid was dissolved in dichloromethane (10−15 mL) and washed with 1 M KOH (2 × 10 mL). The combined organics were dried with magnesium sulfate, filtered through Celite, and dried overnight under vacuum at ambient temperature. The solid was redissolved in THF, and diethyl ether was diffused into the solution to afford red crystals, which were suitable for X-ray diffraction experiments. Analytically pure solid was isolated after heating the solid at 75 °C under vacuum for 4 h (24 mg, 36% yield). Compound **7** could be prepared by an alternate method using 2 equiv of $Ni(OTf)_2$·2MeCN and 6 equiv of Et_4NOH, and washing the product with 1 M NaOH instead of 1 M M KOH (40% yield). IR: 2962 (m), 1675 (m), 1617 (s) 1586 (s), 1453 (s), 1032 (s) cm^{-1}. ^1H NMR (500 MHz, $CDCl_3$) δ ppm 0.11 (m, 57 H), 1.21 (m, 22 H), 1.27 (d, J = 6.73 Hz, 8 H), 2.39 (br s, 12 H), 2.84 (m, 3 H), 2.98 (br q, J = 7.10 Hz, 16 H), 3.13 (m, 4 H), 3.27 (m, 6 H), 3.51 (spt, J = 7.50 Hz, 2 H), 3.66 (spt, J = 7.60 Hz, 2 H), 3.74 (m, 2 H), 6.56 (s, 2 H), 6.59 (d, J = 1.92 Hz, 2 H), 6.79 (d, J = 2.33 Hz, 2 H), 6.81 (d, J = 2.33 Hz, 2 H), 6.91 (d, J = 2.33 Hz, 2 H), 7.00 (d, J = 2.33 Hz, 2 H), 7.51 (d, J = 7.69 Hz, 2 H), 7.54 (d, J = 7.69 Hz, 2 H), 7.70 (d, J = 2.47 Hz, 2 H), 7.78 (t, J = 7.69 Hz, 1 H), 7.84 (t, J = 7.69 Hz, 1 H), 7.99 (t, J = 7.76 Hz, 1 H), 8.27 (d, J = 7.82 Hz, 2 H), 11.32 (s, 2 H). ^{13}C NMR (126 MHz, $CDCl_3$) δ ppm 7.38, 15.38−15.88, 23.57, 23.71, 24.20, 24.43, 24.64, 26.33−26.60, 30.92, 40.19, 53.04, 68.70, 69.73, 69.92, 119.05, 121.45, 121.94, 122.33, 123.86, 125.20, 125.57, 125.67−125.87, 125.91−126.19, 126.69, 132.88, 137.83, 138.03, 138.27, 138.72, 139.09, 140.83, 140.99, 141.38, 141.68, 141.90, 142.17, 150.36−150.52, 151.84−151.94, 152.08, 152.34, 152.57, 159.35, 163.66, 167.72. HRMS-ESI(−): m/z 839.7996, calcd for $[C_{90}H_{99}N_9Ni_2O_{16}]^{2-}$ 839.7964. Anal. Calcd for $C_{106}H_{143}N_{11}Ni_2O_{18}$: C, 64.41; H, 7.29; N, 7.79. Found: C, 64.29; H, 7.26; N, 7.69.

$[Et_4N]_2[(NiOH)_2H_2L]$ (8). A solution of H_6**L** (55 mg, 0.037 mmol) in THF (10 mL) was sparged with N_2 for 30 min, and $Ni(OTf)_2$·2MeCN (36 mg, 0.081 mmol) was added, forming a pale green slurry. Tetraethylammonium hydroxide in methanol (1.5 M, 0.153 mL, 0.229 mmol) was added dropwise to the pale green reaction mixture. Then, the resulting red solution was stirred overnight at room temperature and was dried under reduced pressure for 18 h. The red solid was brought into the glovebox where it was dissolved in THF, filtered through Celite, and dried under reduced pressure.

Reaction of 8 with CO_2. Complex **8** was dissolved in THF (30 mL) in a Schlenk flask to afford a red solution and was freeze−pump−thawed. The solution was stirred for 1 h under a constant pressure of research grade CO_2 that was passed through an O_2 scrubber and two traps immersed in a slurry of liquid nitrogen and chloroform. THF was removed under reduced pressure, and the red solid was then exposed to the atmosphere and dissolved in $CDCl_3$. NMR was collected on the residue indicating the presence of free ligand and **7**.

$[Et_4N]_2[Cu_3(\mu\text{-}\eta^1{:}\eta^2\text{-}OCOO)(\mu\text{-}OH)(OH)H_2L]$ (9). Synthesis of the target complex was carried out on the benchtop with exposure to ambient air. $Cu(OTf)_2$ (79 mg, 0.22 mmol) was added to a solution of H_6**L** (102 mg, 0.0683 mmol) in THF (10−15 mL), after which tetraethylammonium hydroxide (1.5 M in methanol, 0.424 mL, 0.636 mmol) was added dropwise to the reaction mixture. The dark greenish blue reaction mixture was stirred overnight and then filtered through Celite followed by solvent removal from the filtrate under vacuum. The residue was redissolved in dichloromethane (10−15 mL) and extracted with 1 M NaOH (2 × 10 mL). The organic layer was dried with magnesium sulfate, filtered through Celite, and then dried under reduced pressure. The solid was redissolved in THF, and *n*-hexane was diffused into the solution to afford green crystals after 24 h (54.8 mg, 40% yield). IR: 2964 (m), 1672 (m), 1625 (m) 1579 (s), 1450 (s), 1031 (s) cm^{-1}. Evans method ($CDCl_3$): μ_{eff} = 2.80(1) μ_B. HRMS-ESI: m/z 893.2361, calcd for $[C_{90}H_{99}N_9Cu_3O_{17}$, −OH, +Cl$]^{2-}$ 893.2360. Anal. Calcd for $C_{107}H_{142}N_{11}Cl_3Cu_3O_{18}$: C, 59.30; H, 6.60; N, 7.11. Found: C, 58.97; H, 6.60; N, 6.97.

$[Et_4N]_2[Cu(OCOOH)Cu(OH)H_2L]$ (10). Synthesis of the target complex was carried out on the benchtop with exposure to ambient air. $Cu(OTf)_2$ (49 mg, 0.14 mmol) was added to a solution of H_6**L** (101 mg, 0.0676 mmol) in THF (12 mL) followed by tetraethylammonium hydroxide (1.5 M in methanol, 0.413 mL, 0.636 mmol) to afford a dark green mixture. The reaction flask was capped with a septum, and the mixture was stirred overnight and then filtered through Celite, and the filtrate dried under vacuum. The residue was dissolved in dichloromethane (15 mL) and the deep-green solution washed with 1 M KOH (2 × 10 mL). The organics were then dried with magnesium sulfate, the solution filtered through Celite, and filtrate dried under vacuum overnight. The solid was dissolved in THF, and *n*-hexane was diffused into the solution to afford needle-like green crystals (69.5 mg, 52% yield). IR: 2963 (m), 1681 (s), 1586 (s), 1454 (s), 1033 (s) cm^{-1}. Evans method ($CDCl_3$): μ_{eff} = 2.89(1). HRMS-ESI(−): m/z 844.7916, calcd for $[C_{90}H_{99}N_9Cu_2O_{16}]^{2-}$ 844.7913. Anal. Calcd for $C_{106}H_{143}N_{11}Cu_2O_{18}$: C, 64.09; H, 7.26; N, 7.76. Found: C, 63.88; H, 7.20; N, 7.82.

Magnetic Measurements and Data Simulations. Sample preparation, data collection, and simulations were carried out as described previously.[9b] In these simulations, which employed codes written to work with EasySpin[22] running in Matlab, a correction that accounts for underlying temperature independent contributions χ_{dia} and χ_{TIP} was included with value −0.001 38 emu/mol, according to χ_{dia} estimated from Pascal's constants and χ_{TIP} based on reports elsewhere.[33] In addition, a paramagnetic impurity contribution was included in susceptibility and magnetization with S_{free} = 2, g_{free} = 2.03 in form of $(1 - A)\chi_S + A\chi_{free}$ with a value of 0.01 for A.

Mossbauer Spectroscopy. Mössbauer spectra were recorded at 4.2 K, either on a low field Mössbauer spectrometer equipped with a Janis SVT-400 cryostat or on a strong field Mössbauer spectrometer equipped with an Oxford Instruments Spectromag 4000 cryostat containing an 8 T split-pair superconducting magnete4. Both spectrometers were operated in a constant acceleration mode in transmission geometry. The isomer shifts were referenced against that of a room temperature metallic iron foil. Analysis of the data was performed with the program WMOSS (WEB Research).

■ ASSOCIATED CONTENT

Ⓢ Supporting Information

Experimental details, supporting figures, and X-ray crystallographic data in CIF format. This material is available free of charge via the Internet at http://pubs.acs.org.

■ AUTHOR INFORMATION

Corresponding Author

*E-mail: murray@chem.ufl.edu.

DOI: 10.1021/ic502873d
Inorg. Chem. 2015, 54, 2691−2704

Present Address

[⊥]Department of Chemistry and Physics, Armstrong State University, 11935 Abercorn Street, Savannah, GA 31419.

Author Contributions

The manuscript was written through contributions of all authors. All authors have given approval to the final version of the manuscript.

Notes

The authors declare no competing financial interest.

■ ACKNOWLEDGMENTS

The following institutions are acknowledged: NSF CRIF award to the University of Florida (UF) Chemistry Department (CHE-1048604) (L.J.M.); NSF (CHE-0821346) and UF for funding X-ray equipment purchase (K.A.A.); The University of Florida (L.J.M., K.A.A.); ACS Petroleum Research Fund 52704-DNI3 (L.J.M.); Labex ARCANE ANR-11-LABX-0003−01 (R.G.-S.); Fulbright Commission of the Slovak Republic (M.W.M.); APVV-0132-11 and VEGA 1/0145/13 (E.Č.); National Science Foundation (NSF) awards DMR-1202033 (M.W.M.) and DMR-1157490 (NHMFL). Contributions from M.K. Peprah and E.S. Knowles during the early stages of the magnetometry studies are gratefully acknowledged.

■ REFERENCES

(1) (a) Tinberg, C. E.; Lippard, S. J. *Acc. Chem. Res.* **2011**, *44*, 280. (b) Solomon, E. I.; Augustine, A. J.; Yoon, J. *Dalton Trans.* **2008**, 3921. (c) Solomon, E. I.; Heppner, D. E.; Johnston, E. M.; Ginsbach, J. W.; Cirera, J.; Qayyum, M.; Kieber-Emmons, M. T.; Kjaergaard, C. H.; Hadt, R. G.; Tian, L. *Chem. Rev.* **2014**, *114*, 3659. (d) Blomberg, M. R. A.; Borowski, T.; Himo, F.; Liao, R.-Z.; Siegbahn, P. E. M. *Chem. Rev.* **2014**, *114*, 3601. (e) Murray, L. J.; Lippard, S. J. *Acc. Chem. Res.* **2007**, *40*, 466. (f) Baik, M.-H.; Newcomb, M.; Friesner, R. A.; Lippard, S. J. *Chem. Rev.* **2003**, *103*, 2385. (g) Dey, A.; Jiang, Y.; Ortiz de Montellano, P.; Hodgson, K. O.; Hedman, B.; Solomon, E. I. *J. Am. Chem. Soc.* **2009**, *131*, 7869. (h) Gherman, B. F.; Baik, M.-H.; Lippard, S. J.; Friesner, R. A. *J. Am. Chem. Soc.* **2004**, *126*, 2978. (i) Denisov, I. G.; Makris, T. M.; Sligar, S. G.; Schlichting, I. *Chem. Rev.* **2005**, *105*, 2253. (j) Gourlay, C.; Nielsen, D. J.; White, J. M.; Knottenbelt, S. Z.; Kirk, M. L.; Young, C. G. *J. Am. Chem. Soc.* **2006**, *128*, 2164. (k) Jeoung, J.-H.; Dobbek, H. *Science* **2007**, *318*, 1461. (l) Domsic, J. F.; Avvaru, B. S.; Kim, C. U.; Gruner, S. M.; Agbandje-McKenna, M.; Silverman, D. N.; McKenna, R. *J. Biol. Chem.* **2008**, *283*, 30766. (m) Appel, A. M.; Bercaw, J. E.; Bocarsly, A. B.; Dobbek, H.; DuBois, D. L.; Dupuis, M.; Ferry, J. G.; Fujita, E.; Hille, R.; Kenis, P. J. A.; Kerfeld, C. A.; Morris, R. H.; Peden, C. H. F.; Portis, A. R.; Ragsdale, S. W.; Rauchfuss, T. B.; Reek, J. N. H.; Seefeldt, L. C.; Thauer, R. K.; Waldrop, G. L. *Chem. Rev.* **2013**, *113*, 6621. (n) Can, M.; Armstrong, F. A.; Ragsdale, S. W. *Chem. Rev.* **2014**, *114*, 4149. (o) Burgess, B. K.; Lowe, D. J. *Chem. Rev.* **1996**, *96*, 2983. (p) Holm, R. H.; Kennepohl, P.; Solomon, E. I. *Chem. Rev.* **1996**, *96*, 2239. (q) Hoffman, B. M.; Lukoyanov, D.; Yang, Z.-Y.; Dean, D. R.; Seefeldt, L. C. *Chem. Rev.* **2014**, *114*, 4041.

(2) (a) Solomon, E. I.; Sundaram, U. M.; Machonkin, T. E. *Chem. Rev.* **1996**, *96*, 2563. (b) Liu, J.; Chakraborty, S.; Hosseinzadeh, P.; Yu, Y.; Tian, S.; Petrik, I.; Bhagi, A.; Lu, Y. *Chem. Rev.* **2014**, *114*, 4366. (c) Siegbahn, P. E. M.; Blomberg, M. R. A. *Chem. Rev.* **2010**, *110*, 7040.

(3) (a) Nagano, S.; Poulos, T. L. *J. Biol. Chem.* **2005**, *280*, 31659. (b) Dempsey, J. L.; Winkler, J. R.; Gray, H. B. *Chem. Rev.* **2010**, *110*, 7024. (c) Kaila, V. R. I.; Verkhovsky, M. I.; Wikström, M. *Chem. Rev.* **2010**, *110*, 7062.

(4) (a) Christou, G. *Acc. Chem. Res.* **1989**, *22*, 328. (b) Yachandra, V. K.; Sauer, K.; Klein, M. P. *Chem. Rev.* **1996**, *96*, 2927. (c) Lee, S. C.; Holm, R. H. *Chem. Rev.* **2004**, *104*, 1135. (d) Mukhopadhyay, S.; Mandal, S. K.; Bhaduri, S.; Armstrong, W. H. *Chem. Rev.* **2004**, *104*, 3981. (e) Vela, J.; Stoian, S.; Flaschenriem, C. J.; Münck, E.; Holland, P. L. *J. Am. Chem. Soc.* **2004**, *126*, 4522. (f) Venkateswara Rao, P.; Holm, R. H. *Chem. Rev.* **2004**, *104*, 527. (g) Cady, C. W.; Crabtree, R. H.; Brudvig, G. W. *Coord. Chem. Rev.* **2008**, *252*, 444. (h) Sproviero, E. M.; Gascón, J. A.; McEvoy, J. P.; Brudvig, G. W..; Batista, V. S. *Coord. Chem. Rev.* **2008**, *252*, 395. (i) Mukherjee, S.; Stull, J. A.; Yano, J.; Stamatatos, T. C.; Pringouri, K.; Stich, T. A.; Abboud, K. A.; Britt, R. D.; Yachandra, V. K.; Christou, G. *Proc. Natl. Acad. Sci. U.S.A.* **2012**, *109*, 2257. (j) Lee, S. C.; Lo, W.; Holm, R. H. *Chem. Rev.* **2014**, *114*, 3579. (k) Brown, E. C.; York, J. T.; Antholine, W. E.; Ruiz, E.; Alvarez, S.; Tolman, W. B. *J. Am. Chem. Soc.* **2005**, *127*, 13752. (l) York, J. T.; Bar-Nahum, I.; Tolman, W. B. *Inorg. Chem.* **2007**, *46*, 8105.

(5) (a) Stack, T. D. P.; Holm, R. H. *J. Am. Chem. Soc.* **1987**, *109*, 2546. (b) Zhou, J.; Raebiger, J. W.; Crawford, C. A.; Holm, R. H. *J. Am. Chem. Soc.* **1997**, *119*, 6242. (c) Kanady, J. S.; Lin, P.-H.; Carsch, K. M.; Nielsen, R. J.; Takase, M. K.; Goddard, W. A., III; Agapie, T. *J. Am. Chem. Soc.* **2014**, *136*, 14373. (d) Tsui, E. Y.; Tran, R.; Yano, J.; Agapie, T. *Nat. Chem.* **2013**, *5*, 293. (e) Tsui, E. Y.; Kanady, J. S.; Agapie, T. *Inorg. Chem.* **2013**, *52*, 13833.

(6) (a) Feig, A. L.; Lippard, S. J. *Chem. Rev.* **1994**, *94*, 759. (b) Wallar, B. J.; Lipscomb, J. D. *Chem. Rev.* **1996**, *96*, 2625. (c) Proshlyakov, D. A.; Pressler, M. A.; DeMaso, C.; Leykam, J. F.; DeWitt, D. L.; Babcock, G. T. *Science* **2000**, *290*, 1588. (d) Jensen, K. P.; Bell, C. B.; Clay, M. D.; Solomon, E. I. *J. Am. Chem. Soc.* **2009**, *131*, 12155. (e) Wikström, M. *Biochim. Biophys. Acta* **2012**, *1817*, 468. (f) Pinakoulaki, E.; Daskalakis, V.; Ohta, T.; Richter, O.-M. H.; Budiman, K.; Kitagawa, T.; Ludwig, B.; Varotsis, C. *J. Biol. Chem.* **2013**, *288*, 20261.

(7) (a) Cole, A. P.; Root, D. E.; Mukherjee, P.; Solomon, E. I.; Stack, T. D. P. *Science* **1996**, *273*, 1848. (b) Wallar, B. J.; Lipscomb, J. D. *Chem. Rev.* **1996**, *96*, 2625. (c) Du Bois, J.; Mizoguchi, T. J.; Lippard, S. J. *Coord. Chem. Rev.* **2000**, *200*−*202*, 443. (d) Kim, E.; Chufán, E. E.; Kamaraj, K.; Karlin, K. D. *Chem. Rev.* **2004**, *104*, 1077. (e) Lewis, E. A.; Tolman, W. B. *Chem. Rev.* **2004**, *104*, 1047. (f) Mirica, L. M.; Ottenwaelder, X.; Stack, T. D. P. *Chem. Rev.* **2004**, *104*, 1013. (g) Tshuva, E. Y.; Lippard, S. J. *Chem. Rev.* **2004**, *104*, 987. (h) Ohi, H.; Tachi, Y.; Itoh, S. *Inorg. Chem.* **2006**, *45*, 10825. (i) Brown, E. C.; Johnson, B.; Palavicini, S.; Kucera, B. E.; Casella, L.; Tolman, W. B. *Dalton Trans.* **2007**, 3035. (j) Do, L. H.; Hayashi, T.; Moënne-Loccoz, P.; Lippard, S. J. *J. Am. Chem. Soc.* **2010**, *132*, 1273. (k) Friedle, S.; Reisner, E.; Lippard, S. J. *Chem. Soc. Rev.* **2010**, *39*, 2768. (l) Citek, C.; Lyons, C. T.; Wasinger, E. C.; Stack, T. D. P. *Nat. Chem.* **2012**, *4*, 317. (m) Gupta, A. K.; Tolman, W. B. *Inorg. Chem.* **2012**, *51*, 1881. (n) Li, Y.; Soe, C. M. M.; Wilson, J. J.; Tuang, S. L.; Apfel, U.-P.; Lippard, S. J. *Eur. J. Inorg. Chem.* **2013**, *2013*, 2011.

(8) (a) Zinn, P. J.; Powell, D. R.; Day, V. W.; Hendrich, M. P.; Sorrell, T. N.; Borovik, A. S. *Inorg. Chem.* **2006**, *45*, 3484. (b) Zinn, P. J.; Sorrell, T. N.; Powell, D. R.; Day, V. W.; Borovik, A. S. *Inorg. Chem.* **2007**, *46*, 10120. (c) Shook, R. L.; Borovik, A. S. *Chem. Commun.* **2008**, 6095. (d) Graef, T.; Galezowska, J.; Dechert, S.; Meyer, F. *Eur. J. Inorg. Chem.* **2011**, *2011*, 4161. (e) Ng, G. K.-Y.; Ziller, J. W.; Borovik, A. S. *Inorg. Chem.* **2011**, *50*, 7922. (f) Ng, G. K.-Y.; Ziller, J. W.; Borovik, A. S. *Chem. Commun.* **2012**, *48*, 2546.

(9) (a) Guillet, G. L.; Sloane, F. T.; Dumont, M. F.; Abboud, K. A.; Murray, L. J. *Dalton Trans.* **2012**, *41*, 7866. (b) Guillet, G. L.; Sloane, F. T.; Ermert, D. M.; Calkins, M. W.; Peprah, M. K.; Knowles, E. S.; Čižmár, E.; Abboud, K. A.; Meisel, M. W.; Murray, L. J. *Chem. Commun.* **2013**, *49*, 49.

(10) (a) Huang, D.; Holm, R. H. *J. Am. Chem. Soc.* **2010**, *132*, 4693. (b) Huang, D.; Makhlynets, O. V.; Tan, L. L.; Lee, S. C.; Rybak-Akimova, E. V.; Holm, R. H. *Proc. Natl. Acad. Sci. U.S.A.* **2011**, *108*, 1222. (c) Huang, D.; Makhlynets, O. V.; Tan, L. L.; Lee, S. C.; Rybak-Akimova, E. V.; Holm, R. H. *Inorg. Chem.* **2011**, *50*, 10070. (d) Zhang, X.; Huang, D.; Chen, Y.-S.; Holm, R. H. *Inorg. Chem.* **2012**, *51*, 11017. (e) Donoghue, P. J.; Gupta, A. K.; Boyce, D. W.; Cramer, C. J.; Tolman, W. B. *J. Am. Chem. Soc.* **2010**, *132*, 15869. (f) Donoghue, P. J.; Tehranchi, J.; Cramer, C. J.; Sarangi, R.; Solomon, E. I.; Tolman, W. B. *J. Am. Chem. Soc.* **2011**, *133*, 17602. (g) Halvagar, M. R.; Tolman, W. B. *Inorg. Chem.* **2013**, *52*, 8306. (h) Tehranchi, J.; Donoghue, P. J.;

DOI: 10.1021/ic502873d
Inorg. Chem. 2015, 54, 2691−2704

Cramer, C. J.; Tolman, W. B. *Eur. J. Inorg. Chem.* **2013**, *2013*, 4077. (i) Halvagar, M. R.; Neisen, B.; Tolman, W. B. *Inorg. Chem.* **2013**, *52*, 793. (j) Halvagar, M. R.; Solntsev, P. V.; Lim, H.; Hedman, B.; Hodgson, K. O.; Solomon, E. I.; Cramer, C. J.; Tolman, W. B. *J. Am. Chem. Soc.* **2014**, *136*, 7269. (k) Noveron, J. C.; Olmstead, M. M.; Mascharak, P. K. *J. Am. Chem. Soc.* **2001**, *123*, 3247. (l) Marlin, D. S.; Olmstead, M. M.; Mascharak, P. K. *Angew. Chem., Int. Ed.* **2001**, *40*, 4752.

(11) (a) Barrett, A. G. M.; Crimmin, M. R.; Hill, M. S.; Hitchcock, P. B.; Kociok-Köhn, G.; Procopiou, P. A. *Inorg. Chem.* **2008**, *47*, 7366. (b) Appelt, C.; Slootweg, J. C.; Lammertsma, K.; Uhl, W. *Angew. Chem., Int. Ed.* **2012**, *51*, 5911. (c) Horn, B.; Limberg, C.; Herwig, C.; Feist, M.; Mebs, S. *Chem. Commun.* **2012**, *48*, 8243. (d) Thirumoorthi, R.; Chivers, T. *Eur. J. Inorg. Chem.* **2012**, *2012*, 3061. (e) Moore, M.; Gambarotta, S.; Bensimon, C. *Organometallics* **1997**, *16*, 1086. (f) Chisholm, M. H.; Iyer, S. S.; Streib, W. E. *New J. Chem.* **2000**, *24*, 393. (g) Andrews, P. C.; Armstrong, D. R.; Raston, C. L.; Roberts, B. A.; Skelton, B. W.; White, A. H. *J. Chem. Soc., Dalton Trans.* **2001**, 996. (h) Chen, X.; Lim, S.; Plećnik, C. E.; Liu, S.; Du, B.; Meyers, E. A.; Shore, S. G. *Inorg. Chem.* **2005**, *44*, 6052. (i) Layfield, R. A.; García, F.; Hannauer, J.; Humphrey, S. M. *Chem. Commun.* **2007**, 5081.

(12) (a) Korendovych, I. V.; Staples, R. J.; Reiff, W. M.; Rybak-Akimova, E. V. *Inorg. Chem.* **2004**, *43*, 3930. (b) Korendovych, I. V.; Kryatova, O. P.; Reiff, W. M.; Rybak-Akimova, E. V. *Inorg. Chem.* **2007**, *46*, 4197.

(13) (a) de Bruin, B.; Bill, E.; Bothe, E.; Weyhermüller, T.; Wieghardt, K. *Inorg. Chem.* **2000**, *39*, 2936. (b) Gibson, V. C.; Redshaw, C.; Solan, G. A. *Chem. Rev.* **2007**, *107*, 1745.

(14) Taktak, S.; Ye, W.; Herrera, A. M.; Rybak-Akimova, E. V. *Inorg. Chem.* **2007**, *46*, 2929.

(15) Dinger, M. B.; Scott, M. J. *J. Chem. Soc., Perkin Trans. 1* **2000**, 1741.

(16) (a) Yoneda, K.; Adachi, K.; Nishio, K.; Yamasaki, M.; Fuyuhiro, A.; Katada, M.; Kaizaki, S.; Kawata, S. *Angew. Chem., Int. Ed.* **2006**, *45*, 5459. (b) Bao, X.; Leng, J.-D.; Meng, Z.-S.; Lin, Z.; Tong, M.-L.; Nihei, M.; Oshio, H. *Chem.—Eur. J.* **2010**, *16*, 6169.

(17) Burkill, H. A.; Robertson, N.; Vilar, R.; White, A. J. P.; Williams, D. J. *Inorg. Chem.* **2005**, *44*, 3337.

(18) Saalfrank, R. W.; Trummer, S.; Krautscheid, H.; Schünemann, V.; Trautwein, A. X.; Hien, S.; Stadler, C.; Daub, J. *Angew. Chem., Int. Ed.* **1996**, *35*, 2206.

(19) Herbert, D. E.; Lionetti, D.; Rittle, J.; Agapie, T. *J. Am. Chem. Soc.* **2013**, *135*, 19075.

(20) (a) Eames, E. V.; Betley, T. A. *Inorg. Chem.* **2012**, *51*, 10274. (b) Powers, T. M.; Betley, T. A. *J. Am. Chem. Soc.* **2013**, *135*, 12289.

(21) (a) Boudalis, A. K.; Clemente-Juan, J.-M.; Dahan, F.; Tuchagues, J.-P. *Inorg. Chem.* **2004**, *43*, 1574. (b) Kushch, L. A.; Nikolaev, A. V.; Yagubskii, E. B.; Simonov, S. V.; Shibaeva, R. P.; Sadakov, A. V.; Omel'yanovskii, O. E.; Mironov, V. S. *Inorg. Chem. Commun.* **2012**, *21*, 57. (c) Mereacre, V.; Klöwer, F.; Lan, Y.; Clérac, R.; Wolny, J. A.; Schünemann, V.; Anson, C. E.; Powell, A. K. *Beilstein J. Nanotechnol.* **2013**, *4*, 807.

(22) Stoll, S.; Schweiger, A. *J. Magn. Reson.* **2006**, *178*, 42.

(23) (a) Kapoor, R.; Pathak, A.; Kapoor, P.; Venugopalan, P. *Polyhedron* **2006**, *25*, 31. (b) Kapoor, P.; Pannu, A. P. S.; Sharma, M.; Hundal, G.; Kapoor, R.; Hundal, M. S. *J. Coord. Chem.* **2011**, *64*, 256. (c) Ali, A.; Hundal, G.; Gupta, R. *Cryst. Growth Des.* **2012**, *12*, 1308.

(24) (a) Reynolds, R. A., III; Yu, W. O.; Dunham, W. R.; Coucouvanis, D. *Inorg. Chem.* **1996**, *35*, 2721. (b) Higgs, T. C.; Carrano, C. J. *Inorg. Chem.* **1997**, *36*, 291. (c) Handley, D. A.; Hitchcock, P. B.; Leigh, G. J. *Inorg. Chim. Acta* **2001**, *314*, 1. (d) Schweinfurth, D.; Klein, J.; Hohloch, S.; Dechert, S.; Demeshko, S.; Meyer, F.; Sarkar, B. *Dalton Trans.* **2013**, *42*, 6944.

(25) Nefedov, S. E.; Denisova, T. O. *Russ. J. Inorg. Chem.* **2006**, *51*, 1404.

(26) (a) Jubb, J.; Gambarotta, S. *Inorg. Chem.* **1994**, *33*, 2503. (b) Aspinall, H. C.; Tillotson, M. R. *Inorg. Chem.* **1996**, *35*, 2163. (c) Jubb, J.; Scoles, L.; Jenkins, H.; Gambarotta, S. *Chem.—Eur. J.* **1996**, *2*, 767. (d) Kasani, A.; Kamalesh Babu, R. P.; Feghali, K.; Gambarotta, S.; Yap, G. P. A.; Thompson, L. K.; Herbst-Irmer, R. *Chem.—Eur. J.* **1999**, *5*, 577. (e) Korobkov, I.; Gambarotta, S.; Yap, G. P. A. *Organometallics* **2001**, *20*, 2552.

(27) (a) Shirin, Z.; Thompson, J.; Liable-Sands, L.; Yap, G. P. A.; Rheingold, A. L.; Borovik, A. S. *J. Chem. Soc., Dalton Trans.* **2002**, 1714. (b) Wang, D.; Lindeman, S. V.; Fiedler, A. T. *Eur. J. Inorg. Chem.* **2013**, *2013*, 4473.

(28) (a) Rawle, S. C.; Harding, C. J.; Moore, P.; Alcock, N. W. *J. Chem. Soc., Chem. Commun.* **1992**, 1701. (b) Kitajima, N.; Hikichi, S.; Tanaka, M.; Morooka, Y. *J. Am. Chem. Soc.* **1993**, *115*, 5496. (c) Escuer, A.; Vicente, R.; Kumar, S. B.; Solans, X.; Font-Bardía, M.; Caneschi, A. *Inorg. Chem.* **1996**, *35*, 3094. (d) Escuer, A.; Fallah, M. S.; Kumar, S. B.; Mautner, F.; Vicente, R. *Polyhedron* **1998**, *18*, 377. (e) Escuer, A.; Vicente, R.; Kumar, S. B.; Mautner, F. A. *J. Chem. Soc., Dalton Trans.*. **1998**, 3473. (f) Lozano, A. A.; Sáez, M.; Pérez, J.; García, L.; Lezama, L.; Rojo, T.; López, G.; García, G.; Santana, M. D. *Dalton Trans.* **2006**, 3906. (g) Wikstrom, J. P.; Filatov, A. S.; Mikhalyova, E. A.; Shatruk, M.; Foxman, B. M.; Rybak-Akimova, E. V. *Dalton Trans.* **2010**, *39*, 2504. (h) Martínez-Prieto, L. M.; Real, C.; Ávila, E.; Álvarez, E.; Palma, P.; Cámpora, J. *Eur. J. Inorg. Chem.* **2013**, *2013*, 5555.

(29) (a) Looney, A.; Han, R.; McNeill, K.; Parkin, G. *J. Am. Chem. Soc.* **1993**, *115*, 4690. (b) Company, A.; Jee, J.-E.; Ribas, X.; Lopez-Valbuena, J. M.; Gómez, L.; Corbella, M.; Llobet, A.; Mahía, J.; Benet-Buchholz, J.; Costas, M.; van Eldik, R. *Inorg. Chem.* **2007**, *46*, 9098. (c) Troeppner, O.; Huang, D.; Holm, R. H.; Ivanović-Burmazović, I. *Dalton Trans.* **2014**, *43*, 5274. (d) Looney, A.; Parkin, G.; Alsfasser, R.; Ruf, M.; Vahrenkamp, H. *Angew. Chem., Int. Ed.* **1992**, *31*, 92. (e) Zhang, X.; van Eldik, R.; Koike, T.; Kimura, E. *Inorg. Chem.* **1993**, *32*, 5749. (f) Bazzicalupi, C.; Bencini, A.; Bencini, A.; Bianchi, A.; Corana, F.; Fusi, V.; Giorgi, C.; Paoli, P.; Paoletti, P.; Valtancoli, B.; Zanchini, C. *Inorg. Chem.* **1996**, *35*, 5540.

(30) Schmeier, T. J.; Nova, A.; Hazari, N.; Maseras, F. *Chem.—Eur. J.* **2012**, *18*, 6915.

(31) (a) Sletten, J.; Hope, H.; Julve, M.; Kahn, O.; Verdaguer, M.; Dworkin, A. *Inorg. Chem.* **1988**, *27*, 542. (b) Kitajima, N.; Fujisawa, K.; Koda, T.; Hikichi, S.; Moro-oka, Y. *J. Chem. Soc., Chem. Commun.* **1990**, 1357. (c) Mao, Z.-W.; Heinemann, F. W.; Liehr, G.; van Eldik, R. *J. Chem. Soc., Dalton Trans.* **2001**, 3652. (d) Mateus, P.; Delgado, R.; Lloret, F.; Cano, J.; Brandão, P.; Félix, V. *Chem. Eur. J.* **2011**, *17*, 11193.

(32) Powers, T. M.; Gu, N. X.; Fout, A. R.; Baldwin, A. M.; Hernández Sánchez, R.; Alfonso, D. M.; Chen, Y.-S.; Zheng, S.-L.; Betley, T. A. *J. Am. Chem. Soc.* **2013**, *135*, 14448.

(33) Boča, R. In *Magnetic Functions Beyond the Spin-Hamiltonian*; Mingos, D. M. P., Ed.; Springer-Verlag: Berlin/Heidelberg, 2006; Vol. *117*, pp 1−264.

DOI: 10.1021/ic502873d
Inorg. Chem. 2015, 54, 2691−2704